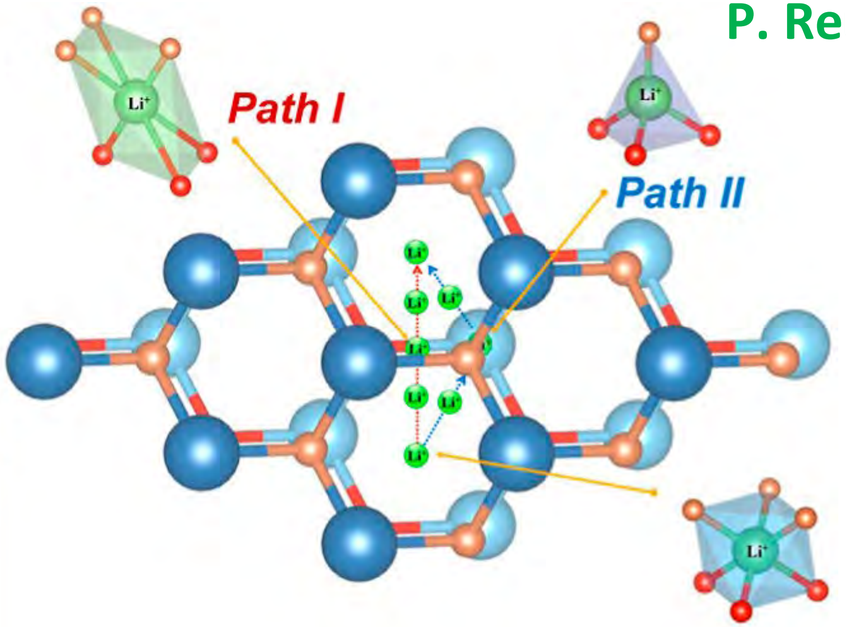
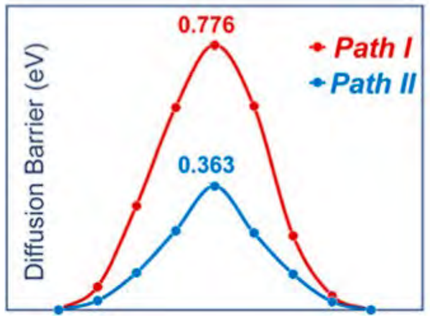
Opening the Way for Lithium: How Atomic-Scale Spacing Controls Ion Transport

T. Sawasdee, T. Kongnok, I. Fongkaew, S. Suthirakun, A. Boonchun,
P. Reunchan, N. Pandech, J. Prasongkit, S. Jungthawan

Co-intercalation yields an ultra-low diffusion barrier for Li atoms



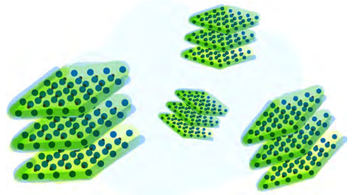


School of Physics, Suranaree University of Technology
Nakhon Ratchasima 30000, THAILAND

Research Outlines

Introduction

Transition metal carbides (MXenes)



Calculation backgrounds

Density functional theory

Self-consistent method used in VASP

Structural morphology and modification

Reviews of their intrinsic property

Synthesis

Applications



Chemical Formula:



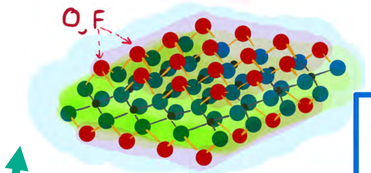


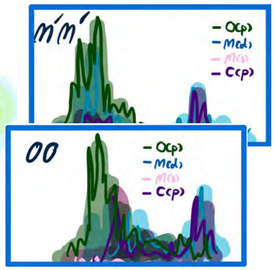
Selection of MXenes with tunable surface functional sites

Studies of monolayer

Structural optimization of M_2CT_2

Electronic properties

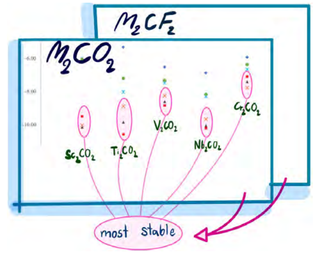




Combination of 3 different surface sites

Density of state (DOS)

Formation energy



A group of preferable structure of the monolayer

Conclusion and Future work

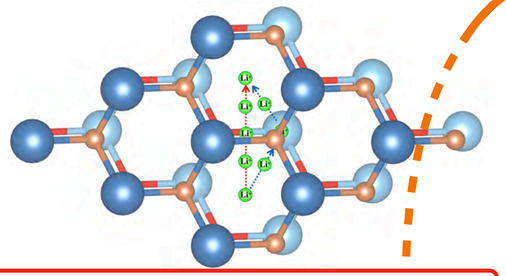
Li-ion applications

Li-ion battery properties of monolayer

Adsorption energy

Open Circuit Voltage

Specific capacitance



Diffusion properties

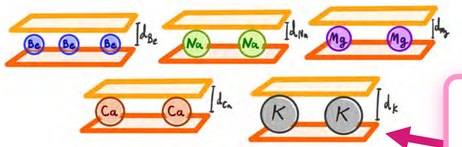
Consideration of interlayer spacing

Diffusion rate and selectivity

Framework for the co-intercalation with Li-diffusion

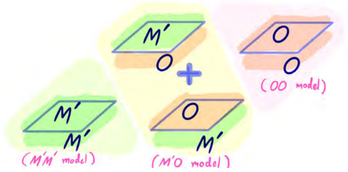
Extension of interlayer spacing

Diffusion rate and selectivity



MXenes bilayer

Construction and Classification of bilayer structures

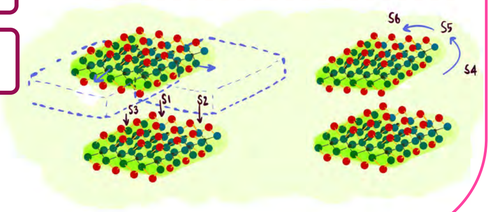


Combination of 2 monolayers

Stacking configurations

Transformation between bilayer's structural forms

translation and rotation

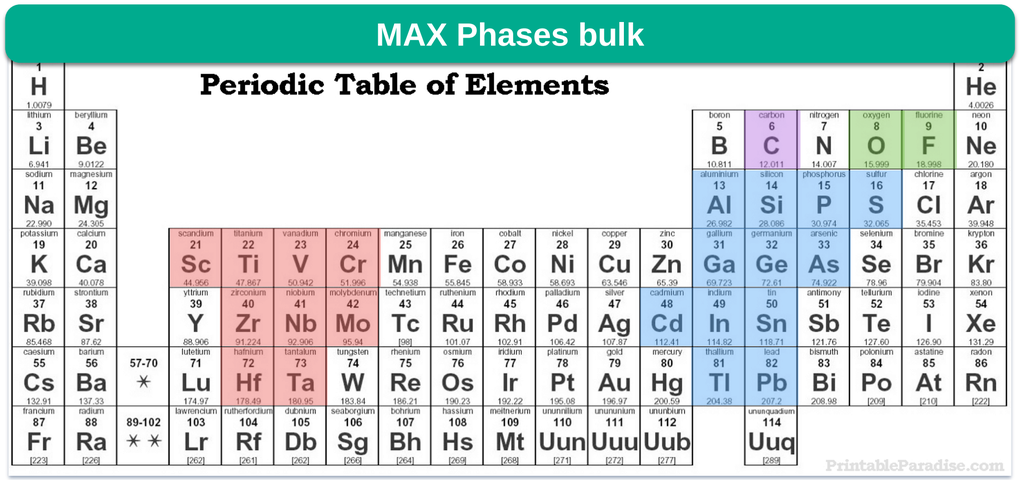


Formation energy

The most stable structural type of MXenes bilayer

I. INTRODUCTION : First Time Synthesized of MXenes by Naguib et. al

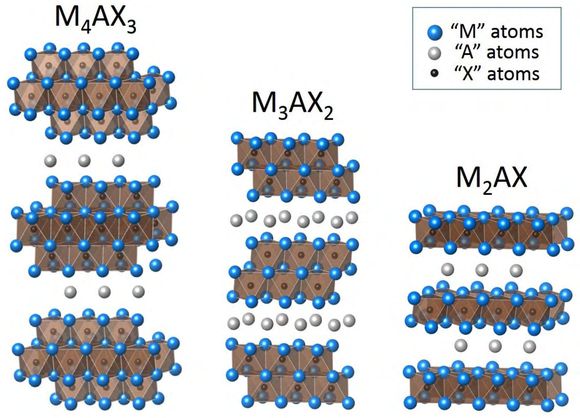
MAX Phases bulk

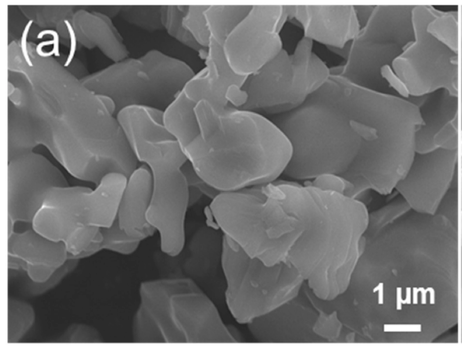


M : Early transition metals
A : Groups 3A, 4A, 5A, 6A
X : C
T : O, F
n : 1, 2, and 3
T_x : Surface functional group; OH, O, F

MAX bulk

$M_{n+1}AX_n$



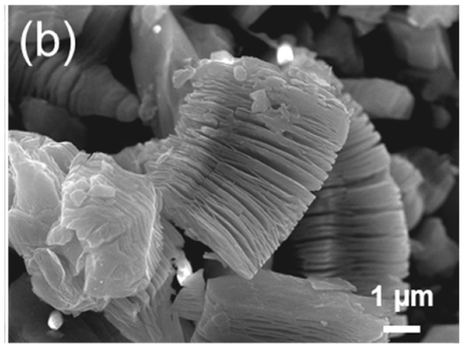


MAX-phase : Ti_3AlC_2

remove A by HF

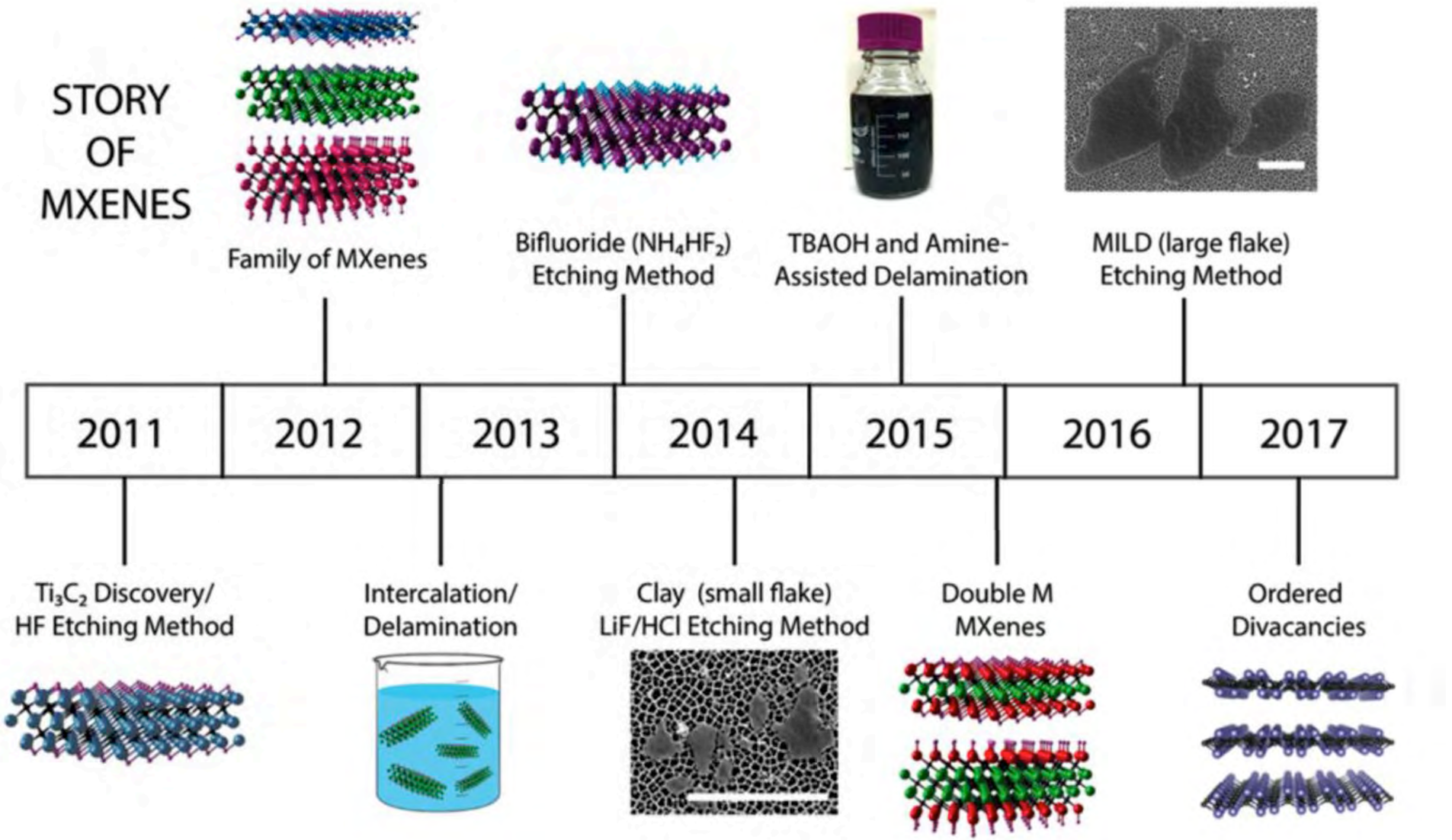
MXenes

$M_{n+1}C_nT_x$ (*n = 1,2,3*)



MXene : $Ti_3C_2T_x$

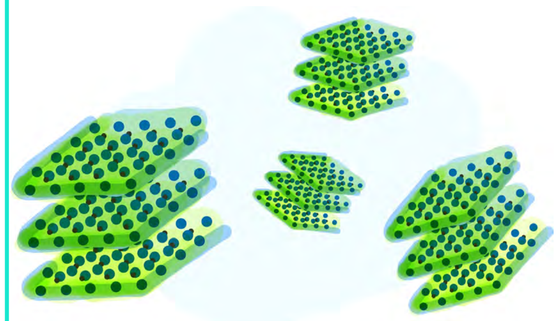
Naguib, M., Advanced Materials 23: 4248 (2011)
Lashgari, H. et al.,Solid State Communications 195: 61.(2014)

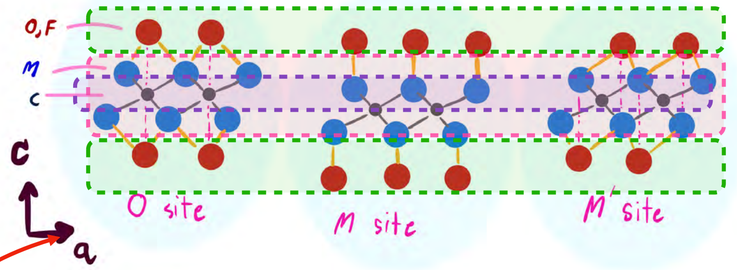


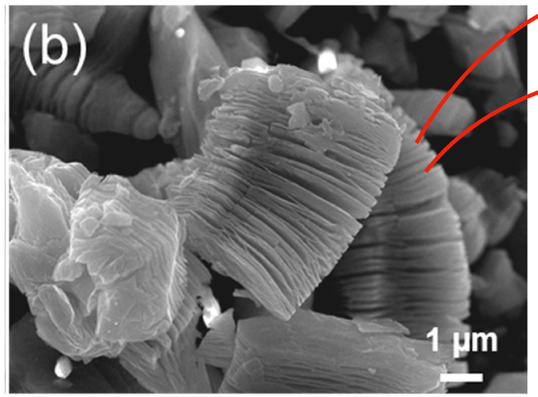
Alhabeb, M. (2017). Guidelines for Synthesis and Processing of Two-Dimensional Titanium Carbide (Ti3C2Tx MXene). **Chemistry of Materials** 29: 7633

I. Introduction : Structural properties

Tunable structure of the material





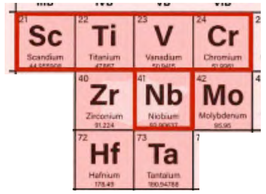


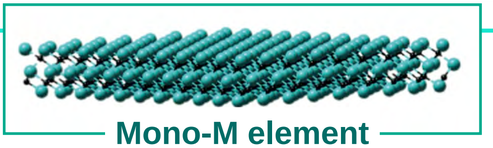
MXene : $Ti_3C_2T_x$

Elemental composition

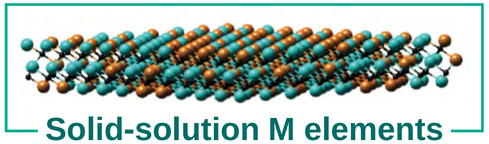
$M_{n+1}X_nT_x$

① **Transition metals (*M*)**

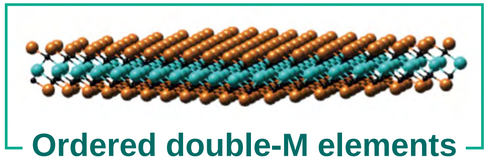




Mono-M element

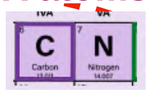


Solid-solution M elements



Ordered double-M elements

② **X atoms**

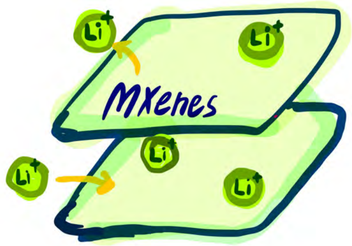


③ ***n*-ordering of M atom**

M_2X, M_3X_2, M_4X_3, M_5X_4

④ **Surface functional groups**



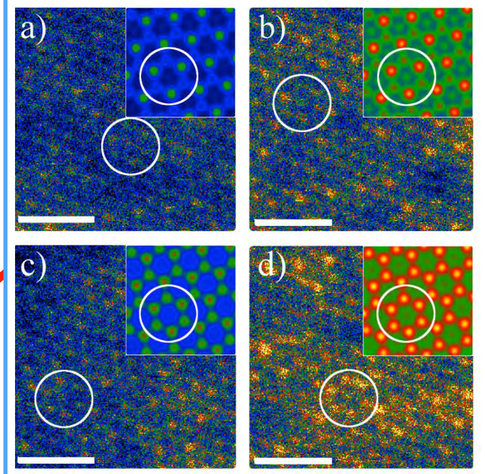


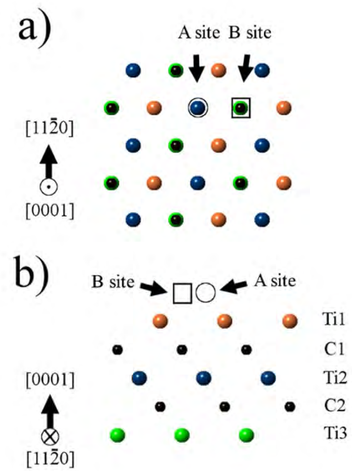
Layered Morphology

Large interlayer spacing

Strong adsorption properties

Anode material for Li-ion battery (LIBs)





Persson, I., et al., 2D Materials 5.(2017)

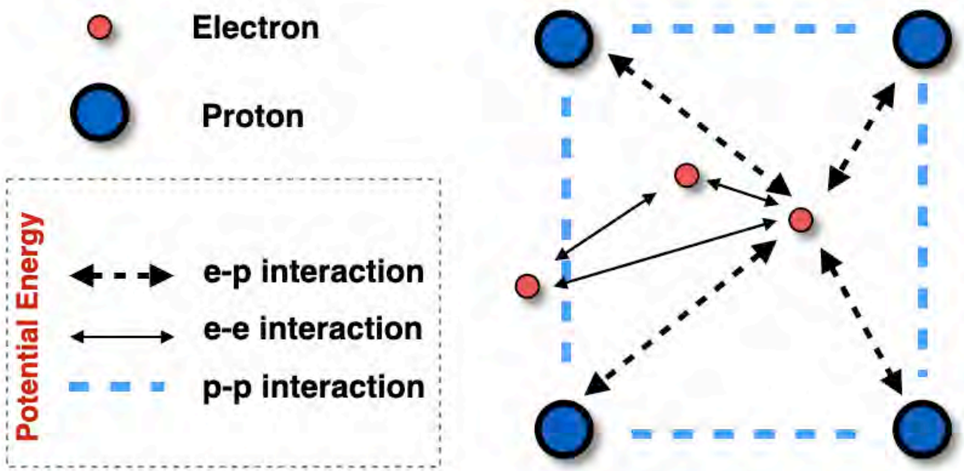
Improve MXenes multilayer for the LIBs



Density functional theory (DFT)

① For any external potential, there is a unique ground state electronic density

Quantum mechanics



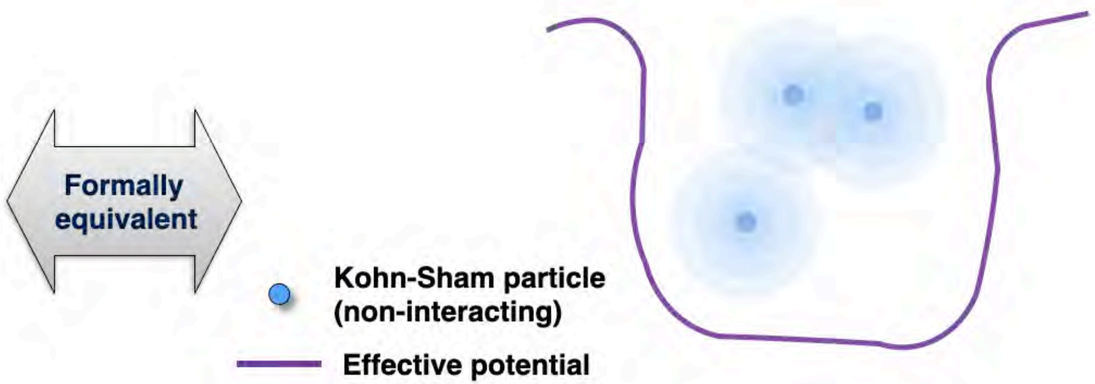
Schrödinger equations

$$\left(\frac{1}{2}\nabla^2 + V(\vec{r})\right)\Psi_i(\vec{r}) = \varepsilon_i \Psi_i(\vec{r})$$

Hohenberg Kohn theorem

② This implies that the ground state electronic density determines all the properties of the system

Density functional theory (DFT)



Kohn-Sham equations

$$\left(\frac{1}{2}\nabla^2 + V_{eff}(\vec{r})\right)\Psi_i(\vec{r}) = \varepsilon_i \Psi_i(\vec{r})$$

Exchange-correlation

$$V_{eff}(\vec{r}) = V_{ext}(\vec{r}) + \int \frac{\rho(\vec{r}\,')}{|\vec{r}\,' - \vec{r}|} d^3r' + v_{xc}(\vec{r})$$

Electrons(Charges) density :

$$\rho(\vec{r}) = \sum_i |\psi_i(\vec{r})|^2$$

Total Energy that is functional of the electron density :

$$E(\rho) = \int \psi_i^*(\vec{r})(-\frac{1}{2}\nabla^2)\psi_i(\vec{r})d^3\vec{r} + \int \rho(\vec{r})v_{ext}(\vec{r})d^3r + \frac{1}{2}\iint \frac{\rho(\vec{r})rho(\vec{r'})}{|\vec{r} - \vec{r'}|} d^3r'd^3r + E_{xc}(\rho)$$

Computational resources

First-principle calculations



a.High Performance Computer Cluster (2.2 GHz, 504 CPUs), operating on Rocks Cluster, at SLRI

b.Institute of Science (IOS) High-performance computer (HPC) at SUT

Input :

Simulation Informations

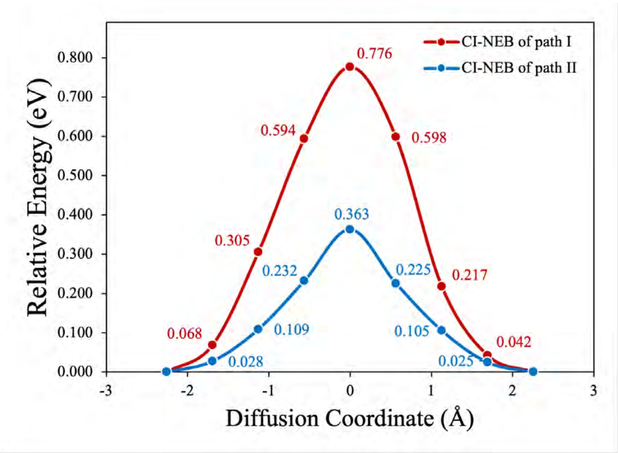
b-initio VASP ienna ackage imulation

Total Energy,

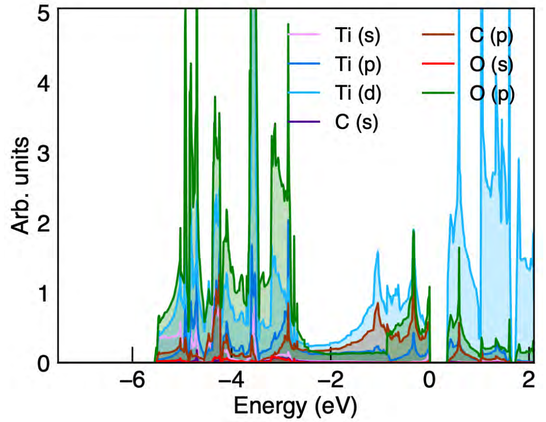
Wave function(ψ), Charge density(ρ),

Formation energy

Diffusion barrier



DOS, Electronic structure



Self-consistent scheme used in VASP



Ionic steps

Electronic steps

Crystal Structure and Calculation Conditions

1 trial-charge ρ_{in} and trial-wavevectors ϕ_n

2 hartree-and XC-potential and d.c.

set up Hamiltonian

3 subspace-diagonalization $\phi_{n'} \Leftarrow U_{n'n}\phi_n$

iterative diagonalization, optimize ϕ_n

subspace-diagonalization $\phi_{n'} \Leftarrow U_{n'n}\phi_n$

4 new partial occupancies f_n

new (free) energy $E = \sum_n \varepsilon_n f_n - d.c. - \sigma S$

5 new charge density $\rho_{out}(r) = \sum_n f_n |\phi_n(r)|^2$

mixing of charge density $\rho_{in}, \rho_{out} \Rightarrow new\rho_{in}$

$\Delta E < E_{break}$

minimized energy, optimized charge density, etc.

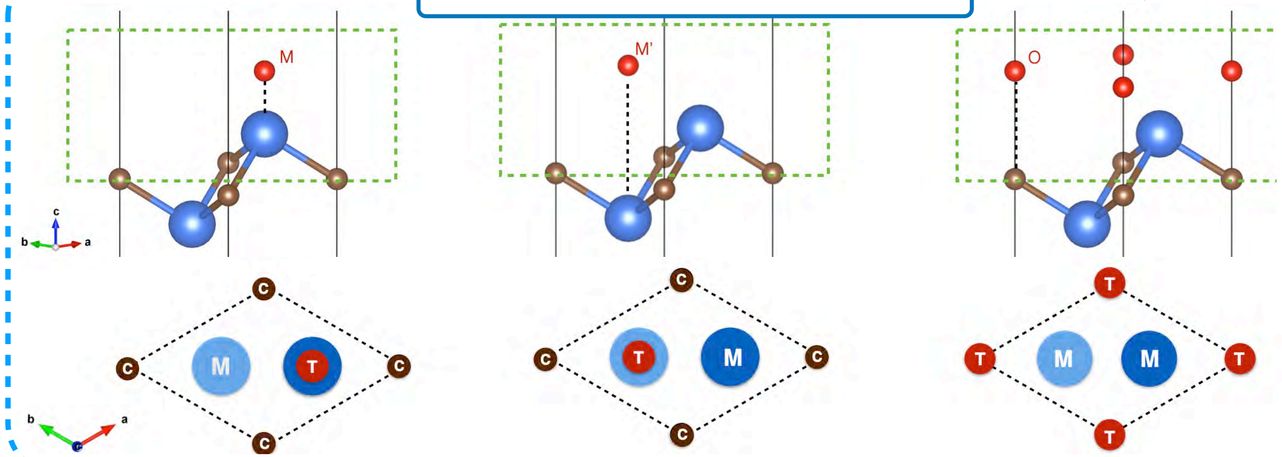
$\Delta F < F_{break}$

update the ion location

Structural Optimization

II. Studies of MXenes monolayers

Structural optimizations



Models

MM M'M' OO

MM' MO M'O

+

Compounds

M_2CT_2

M	T
Sc Ti V Nb Cr	O & F

10 compounds

Structural optimizations

- Includes van der Waals interaction
- Optimization of the structures
- Optimization of their precursor and O and F molecules

(M_2C, T_x)

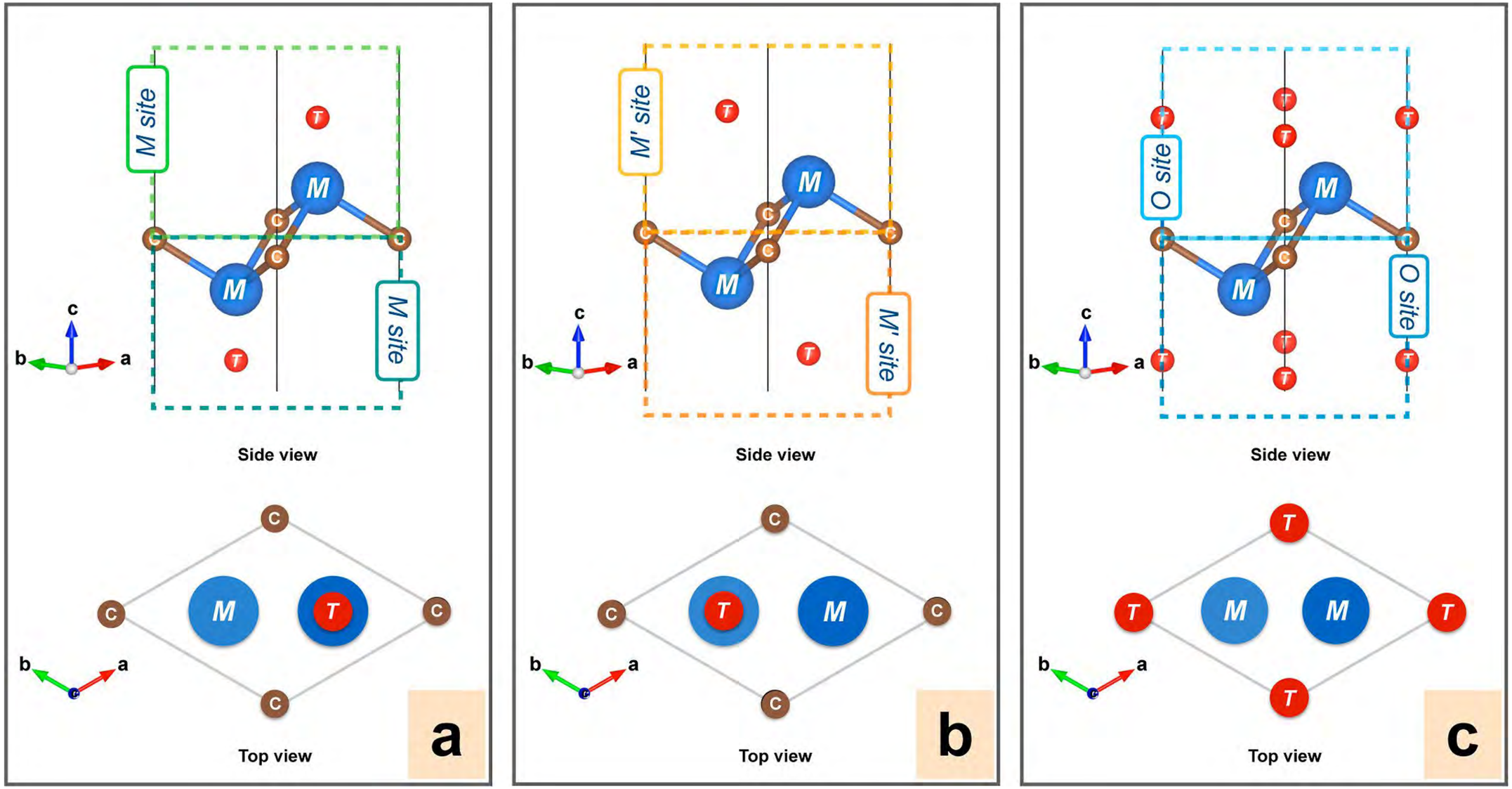
Electronic properties & Stability

Formation Energy

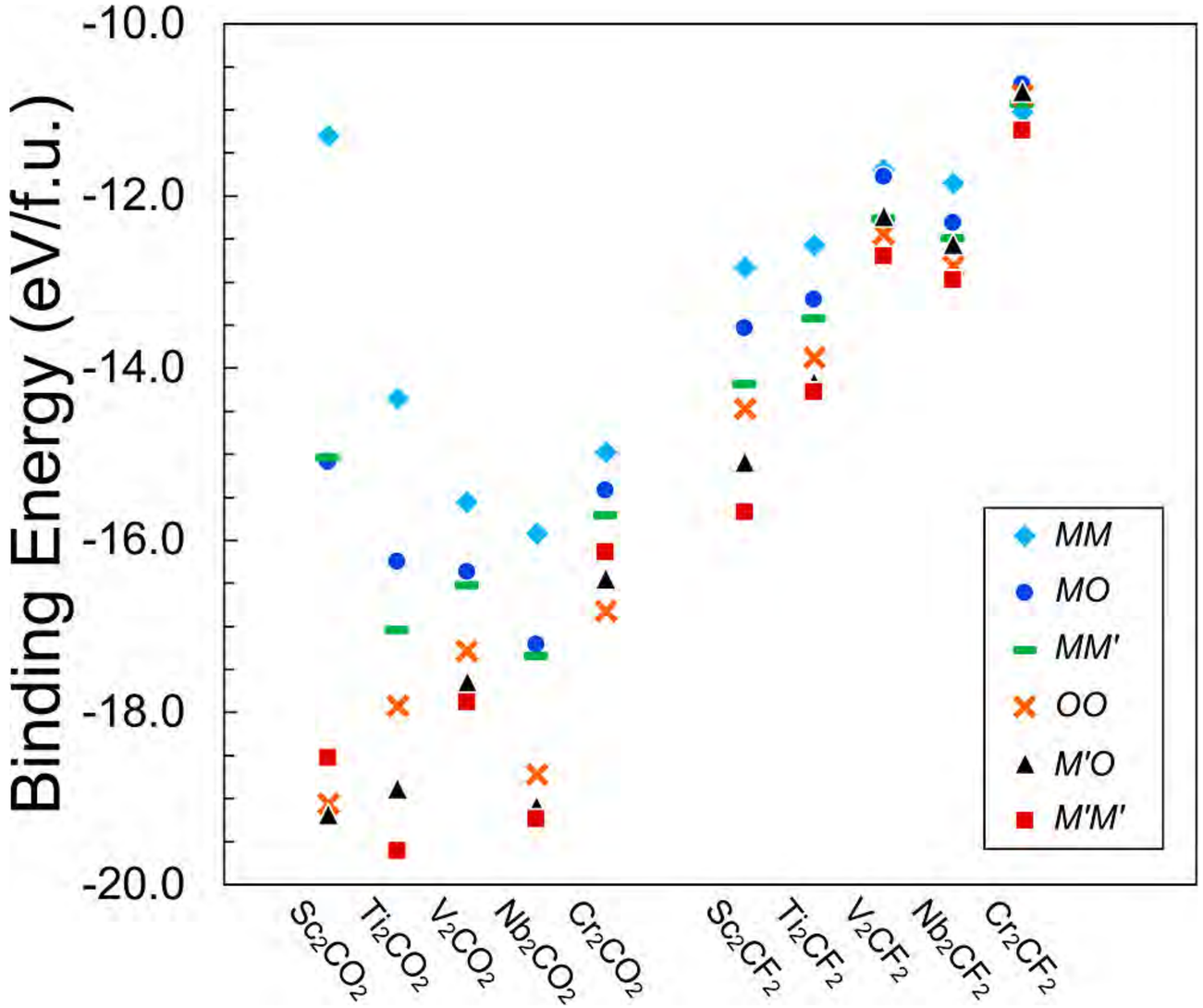
$$E_f^{M_2CT_2} = E^{M_2CT_2} - E^{M_2C} - 2\frac{E^{T_x}}{x}$$

Density of state

- Increase *k*-mesh in the calculations
- Static self-consistency


M site
M
M
C
T
M site
c
b
a
Side view
C
M
T
C
C
b
a
Top view
a
M' site
M
M
C
T
M' site
c
b
a
Side view
C
T
M
C
C
b
a
Top view
b
O site
M
M
C
T
O site
c
b
a
Side view
T
M
M
T
T
b
a
Top view
c

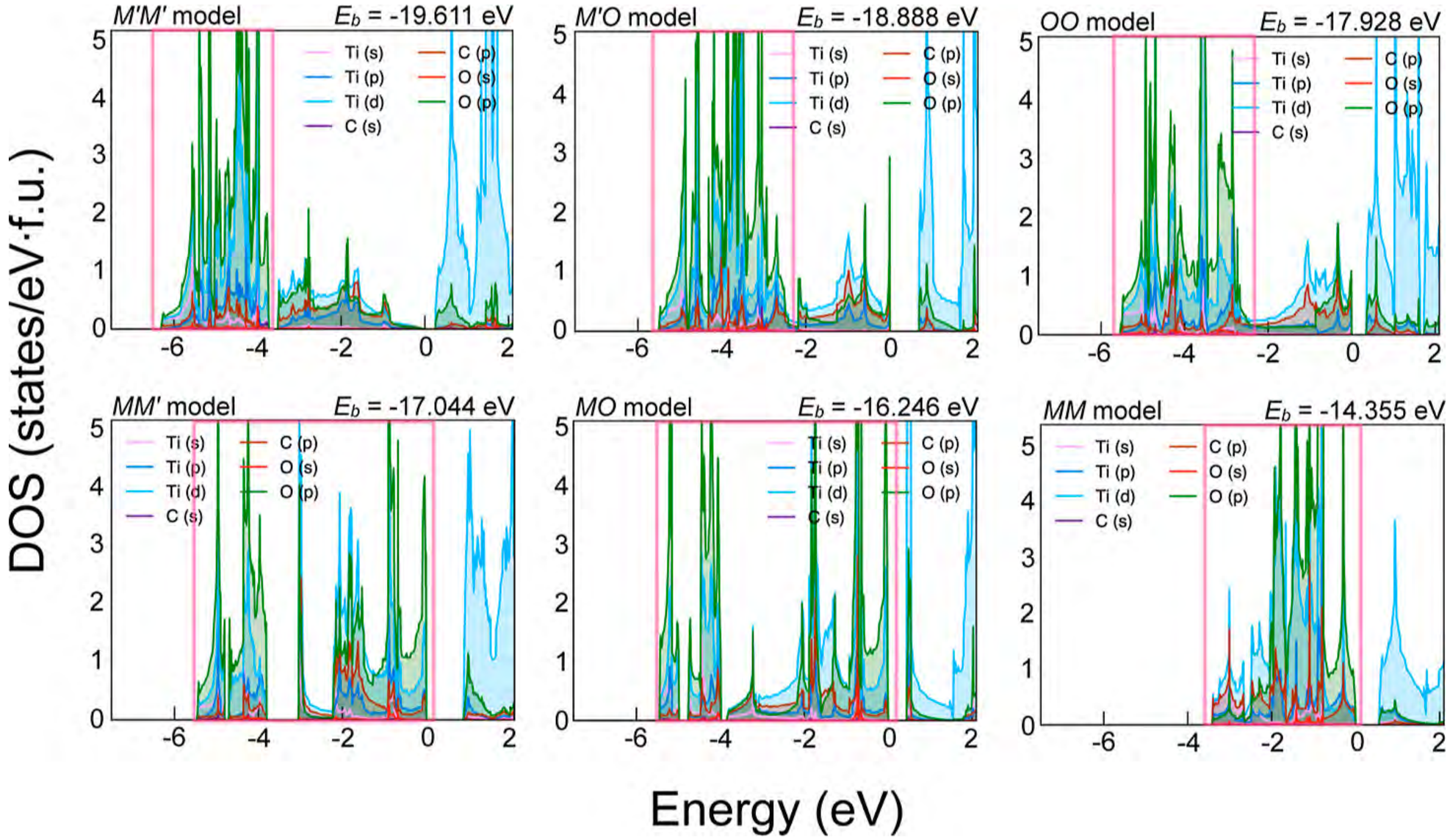
Studies of MXenes monolayers : Formation energy of M_2CT_2 monolayer



***M'M'*, *M'O*, and *OO* models are selected**

The most stable among M_2CO_2 and M_2CF_2 molecules are those with a balanced charge state, such as Ti_2CO_2 and Sc_2CF_2.

Studies of MXenes monolayers : DOS of Ti_2CO_2



Studies of MXenes monolayers : Discussion of DOS

- The calculated DOS shows that the states of O *2p* and *M 3d* hybridization orbitals of the *M'M'* model have a tendency of the highly occupied states in lower energy region than the other models for almost of the interested compounds.

- This indicates that the formation energy of the *M'M'* model is favorable among the studied configurations

- Moreover, the Semiconductor such as Sc_2CO_2, and Ti_2CO_2 structure show the feature of DOS more obviously than the metal.

- The plotting of the E_F have trend of lower energy as shorter O-O distance or the thinness of the M_2CT_2 structure that follow the trend in a similar way of O-O distance in CO_2 molecule.

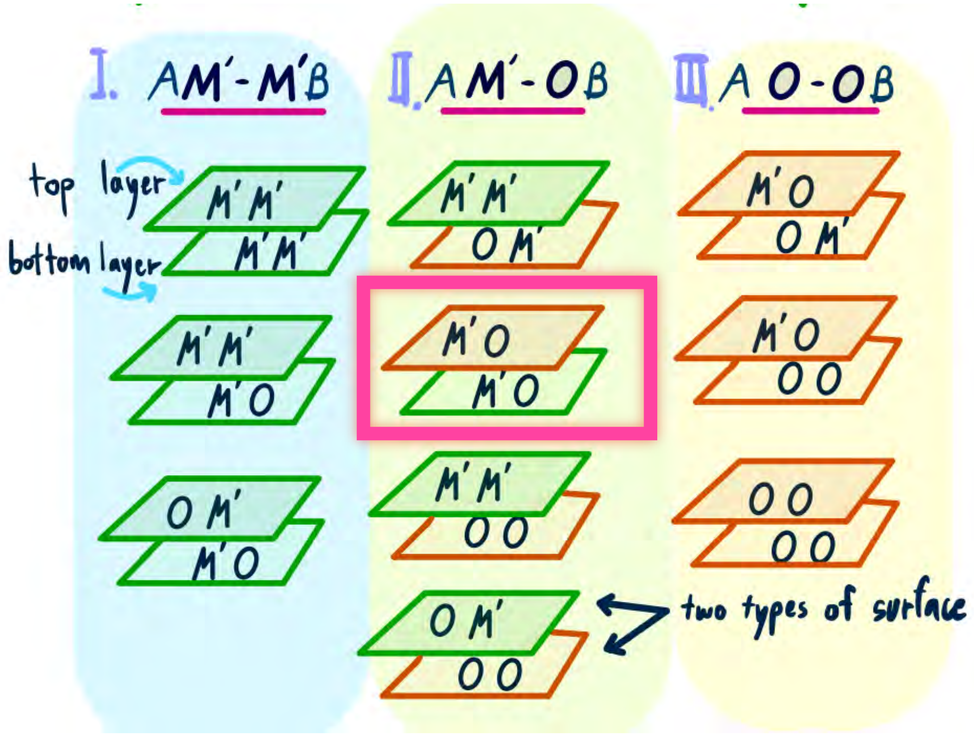
Structural parameter

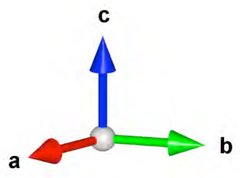
Bilayer structure of M_2CO_2 compound

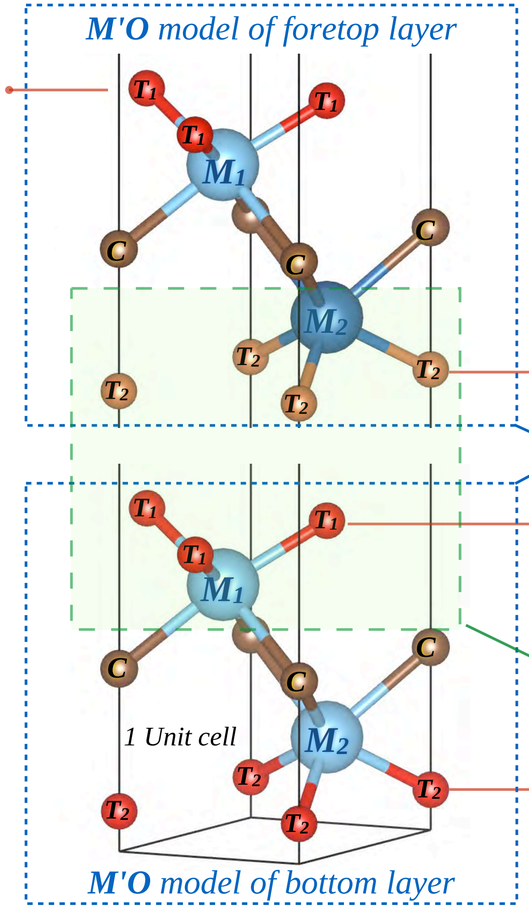
Study of 10 compounds "*c*"

10 numbers of bilayer's combined types "*t*"

6 number of stacking configurations "*s*"







T_1 atom on the M' position of top surface

T_2 atom on the O position of bottom surface

$M'O$-$M'O$ type of bilayer

T_1 atom on the M' position of top surface

"s_5" of bilayer stacking configuration

T_2 atom on the O position of bottom surface

$X_{c,\,t,\,s}$ (POSCAR)

$X_{\,c=2,\,t=5,\,s=5}$

III. MXenes bilayer : bilayer's structural optimizations

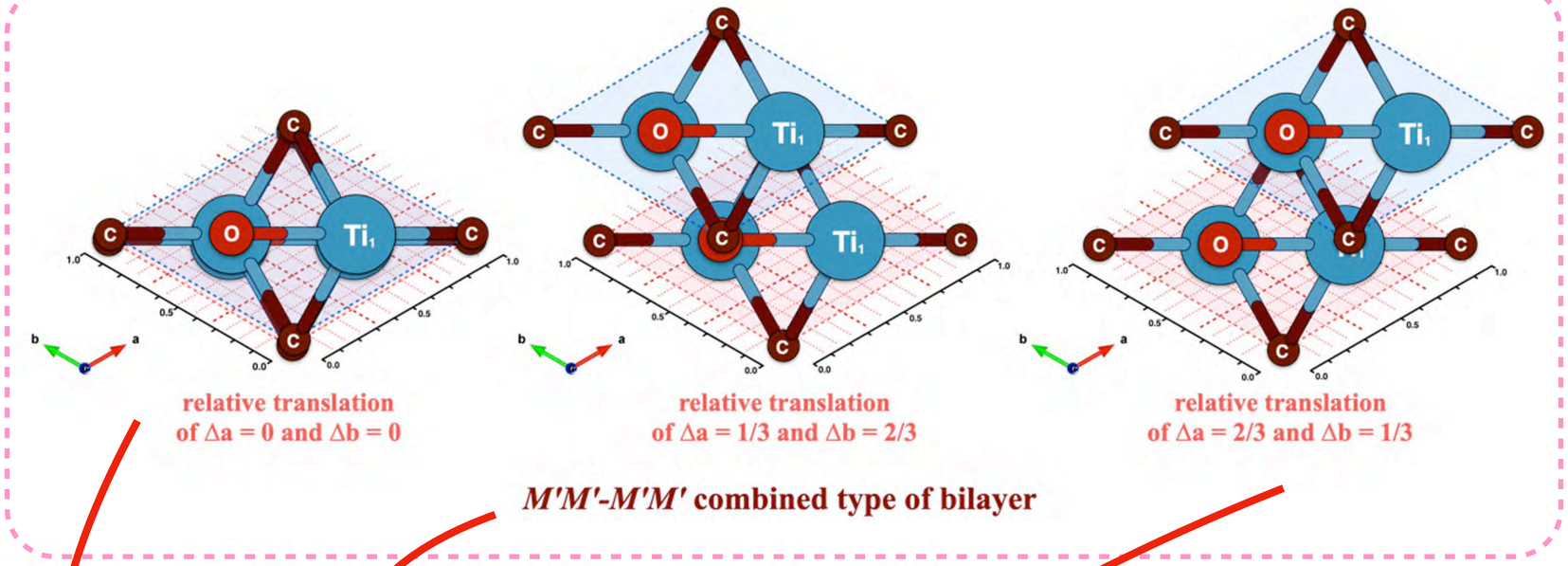
Energy landscape

- Sc_2CO_2
- Ti_2CO_2
- V_2CO_2

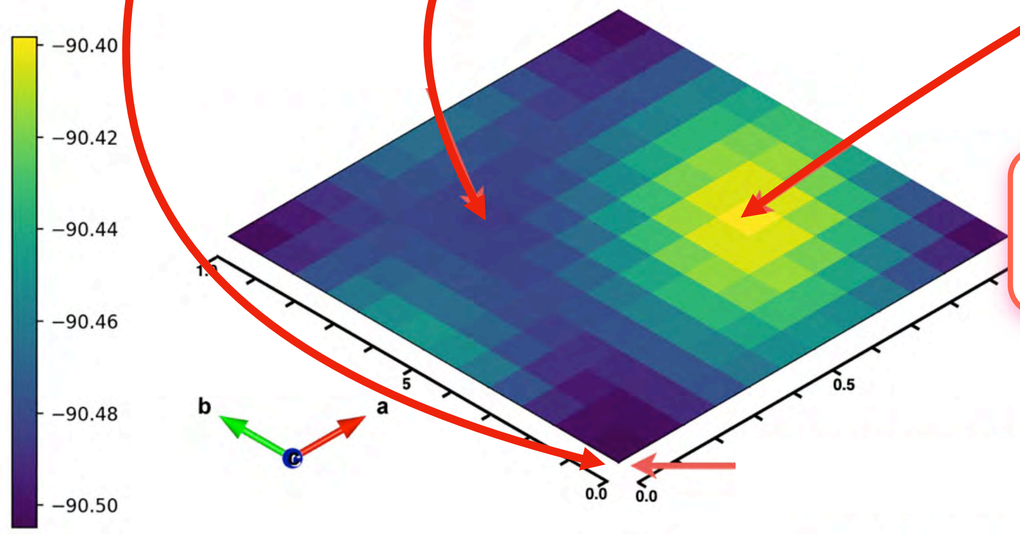
OO-OO

MM'-M'M

M'O-M'O



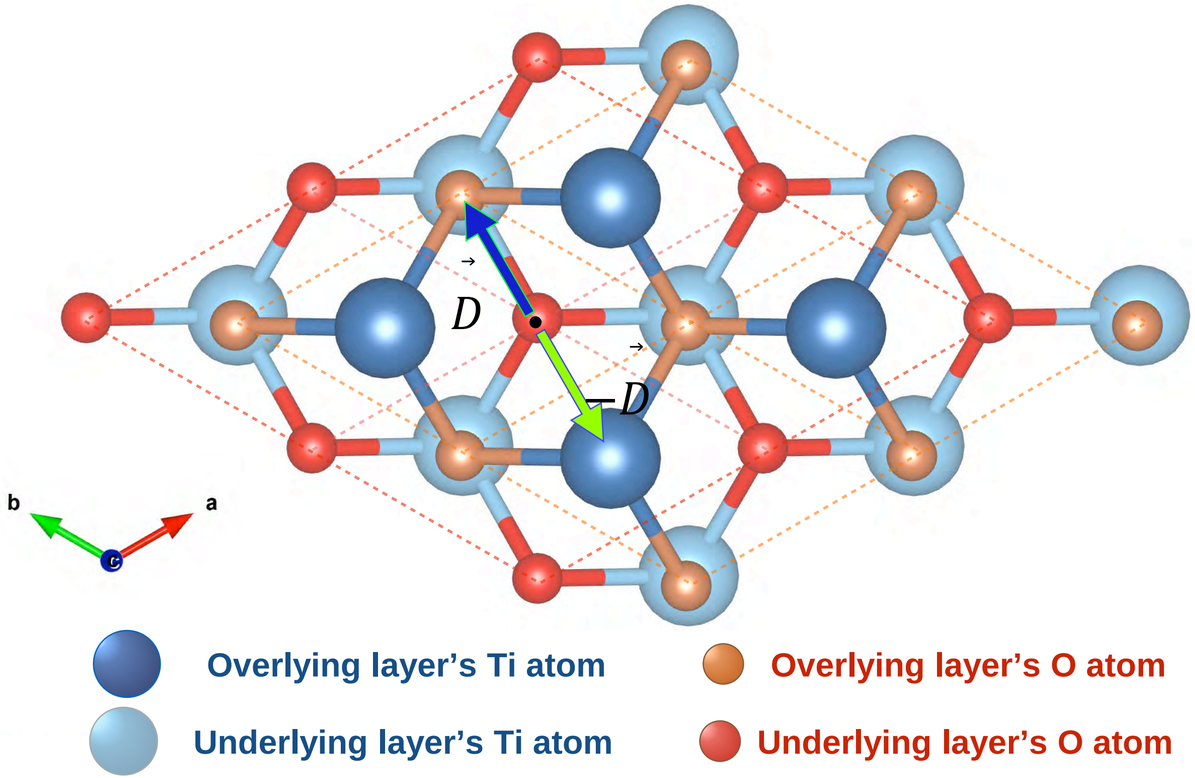
Energy profiles of the *M'M'-M'M'* combined type of the bilayer Ti_2CO_2



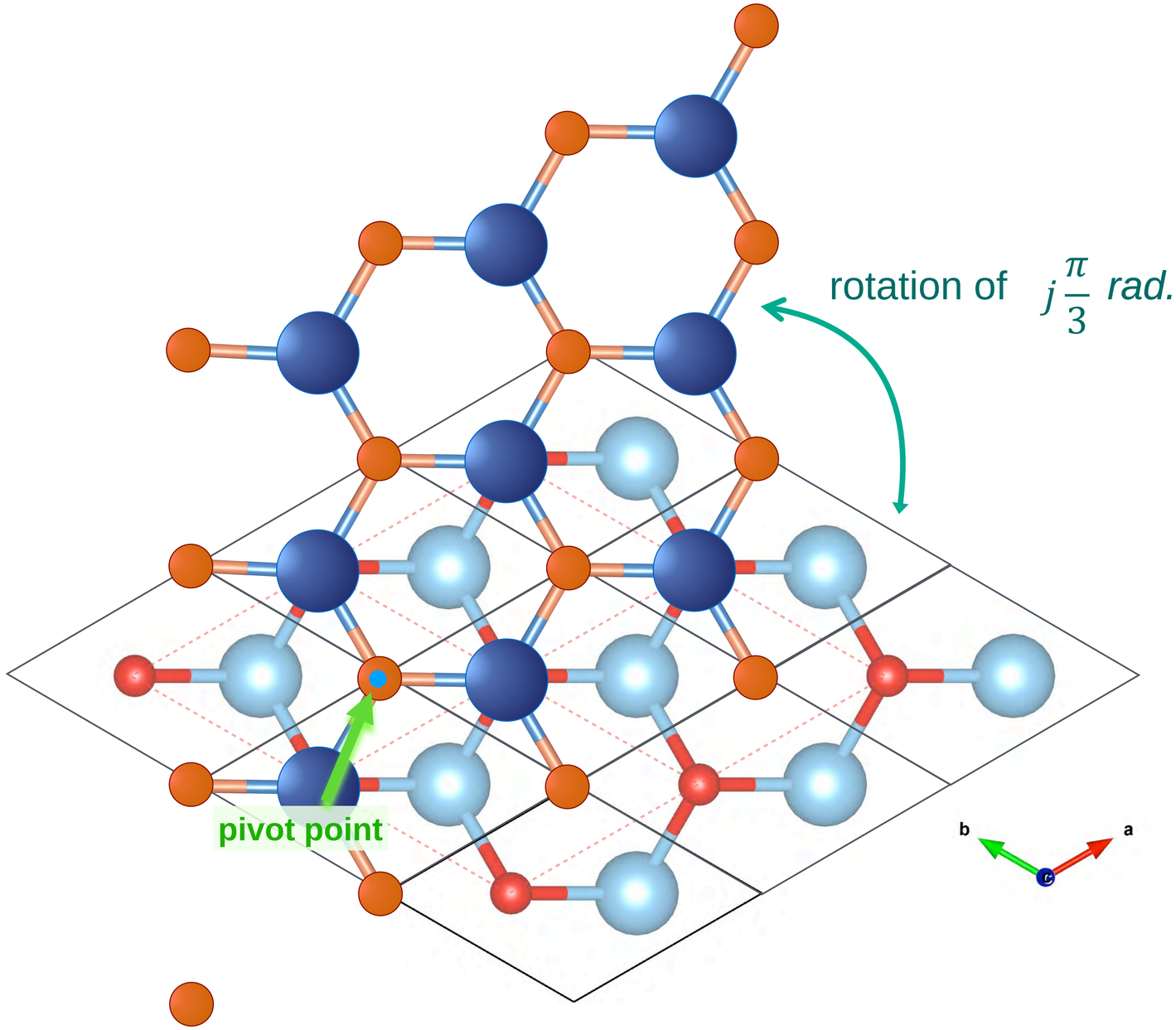
3 symmetric points are discovered

MXenes bilayer : Stacking configurations

Translation vectors



MXenes bilayer : Stacking configurations



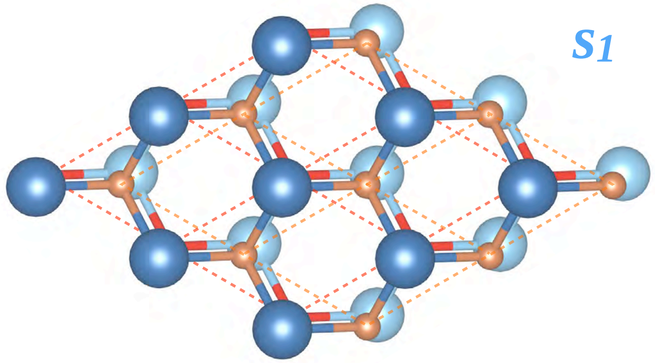
III. MXenes bilayer : Stacking configurations

Overlying layer's Ti atom

Underlying layer's Ti atom

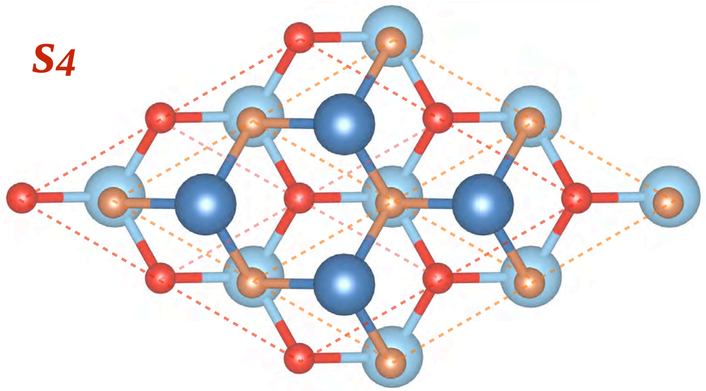
Overlying layer's O atom

Underlying layer's O atom

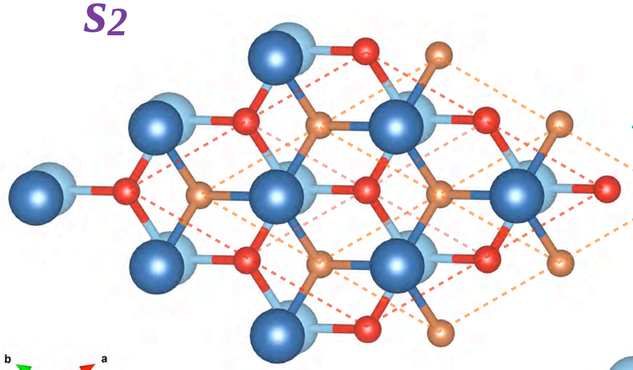


S_1

rotation of $j\frac{\pi}{3}$ *rad.*

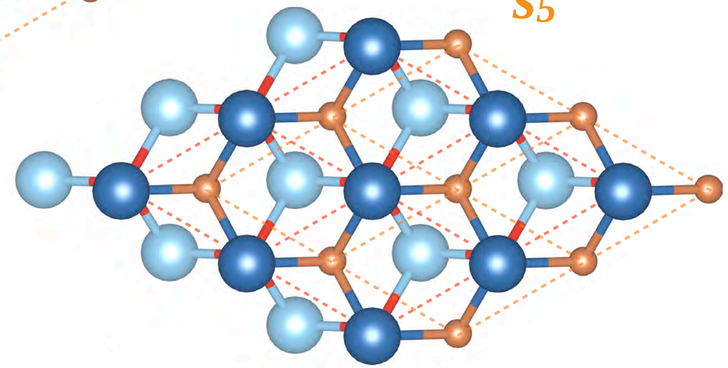


S_4

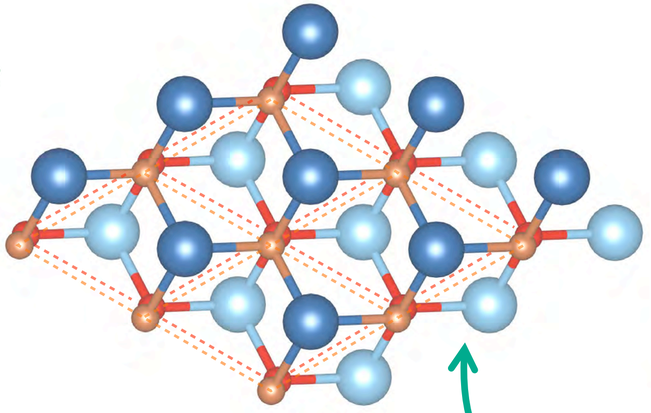


S_2

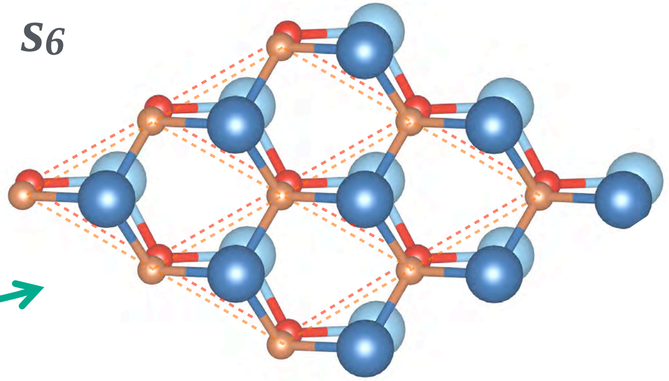
rotation of $j\frac{\pi}{3}$ *rad.*



S_5



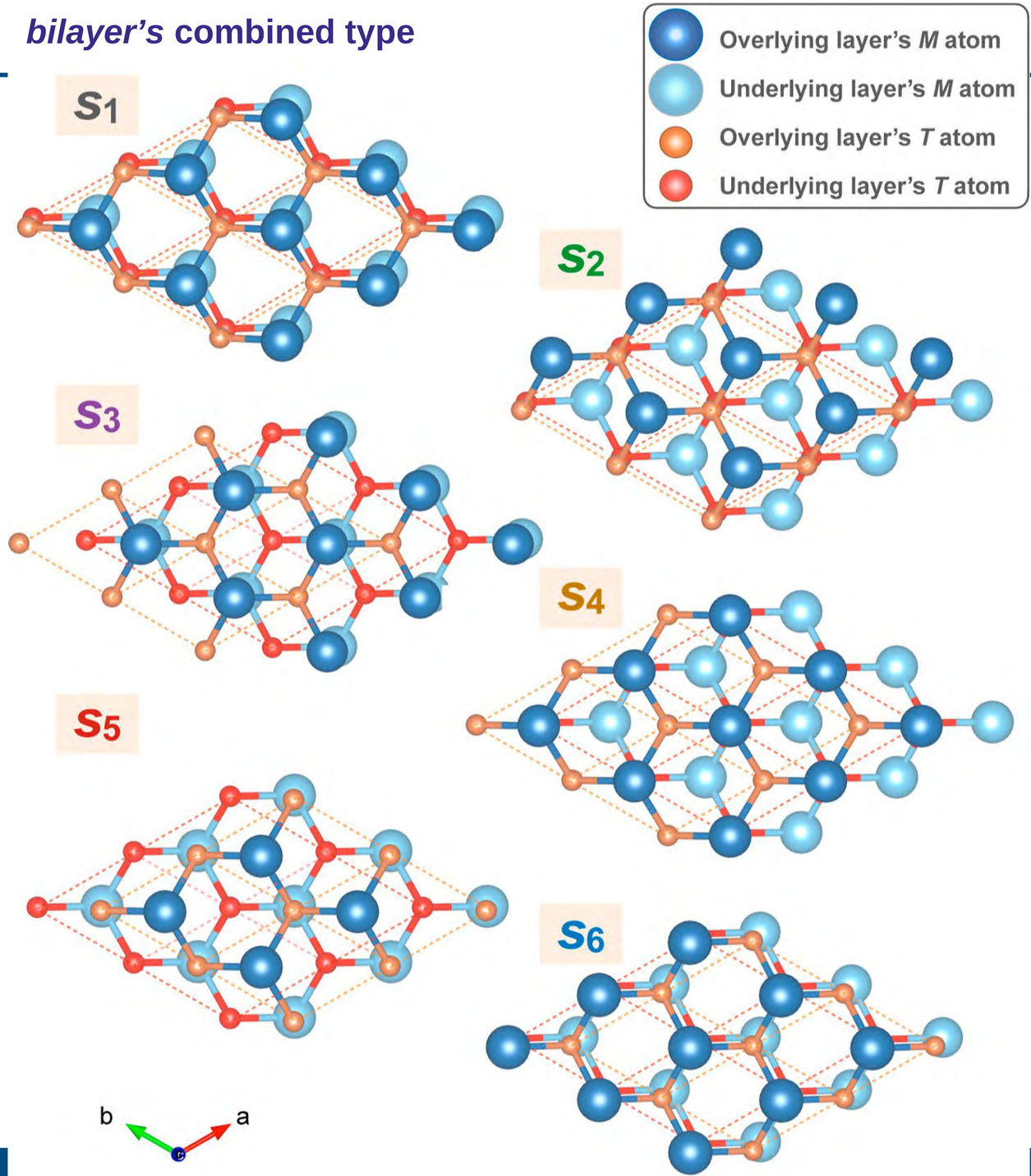
S_3



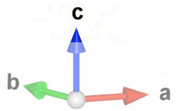
S_6

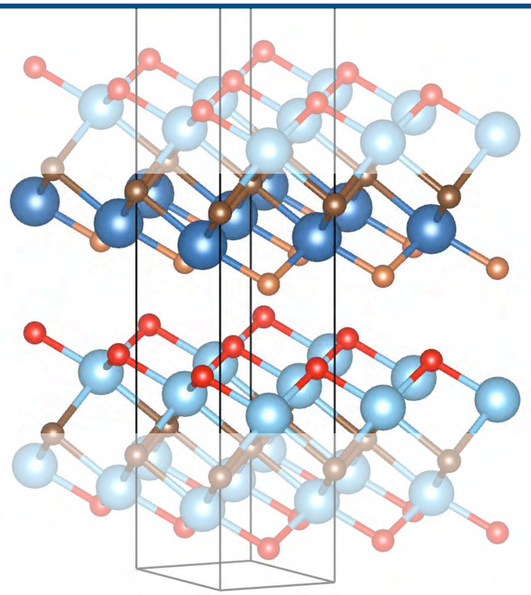
rotation of $j\frac{\pi}{3}$ *rad.*

bilayer's combined type

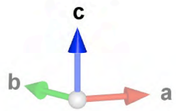


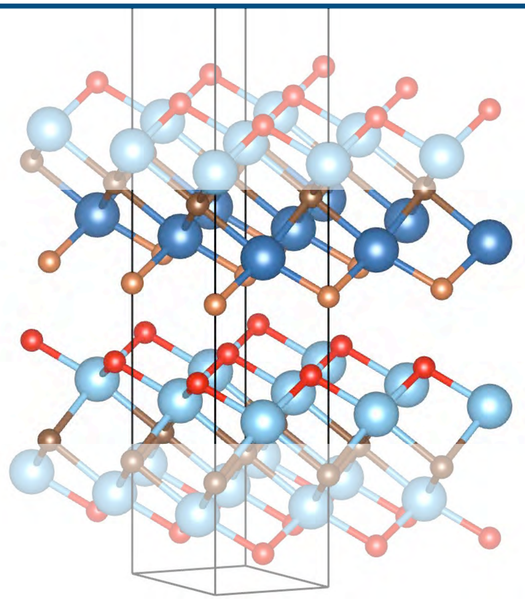
S1



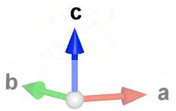


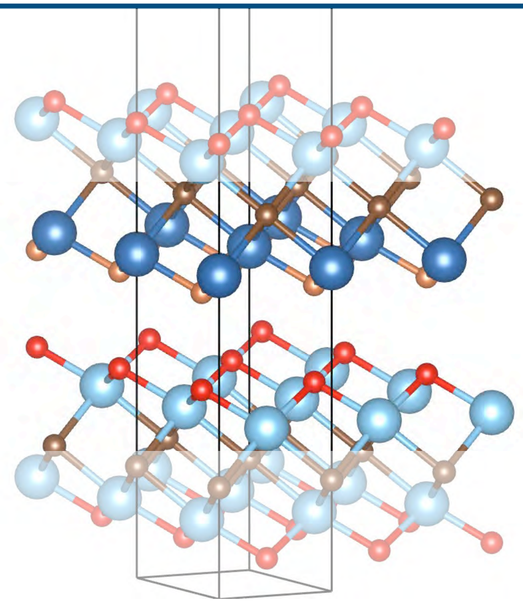
S2



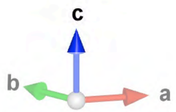


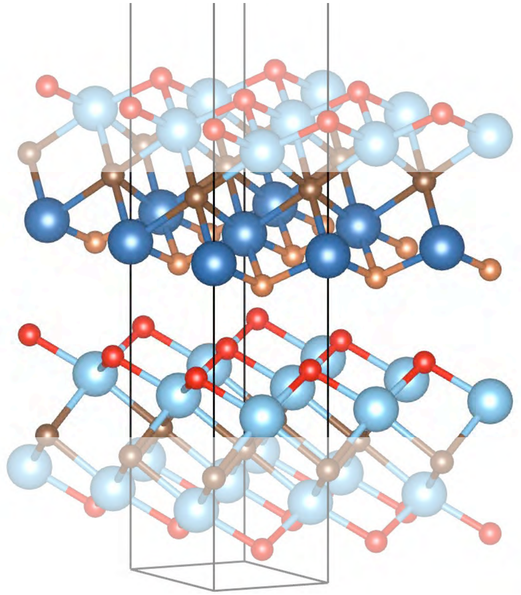
S3



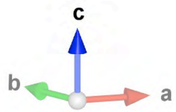


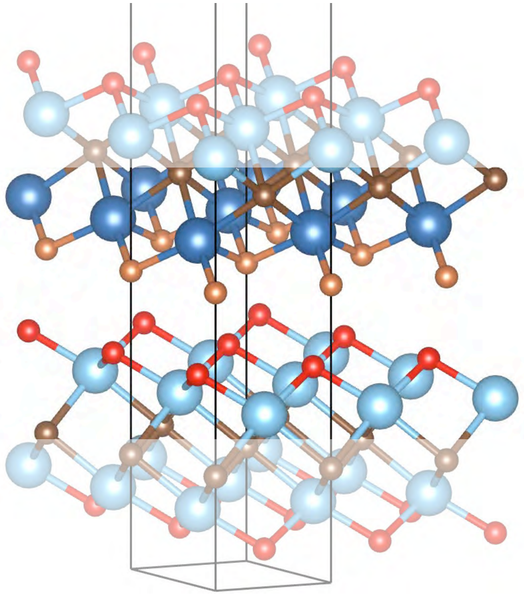
S4



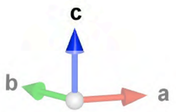


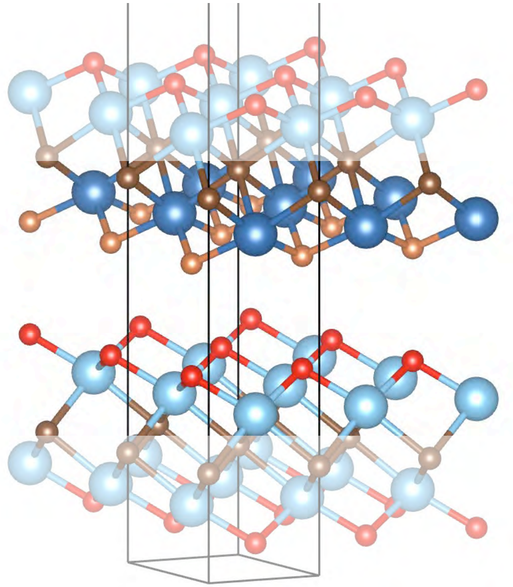
S5



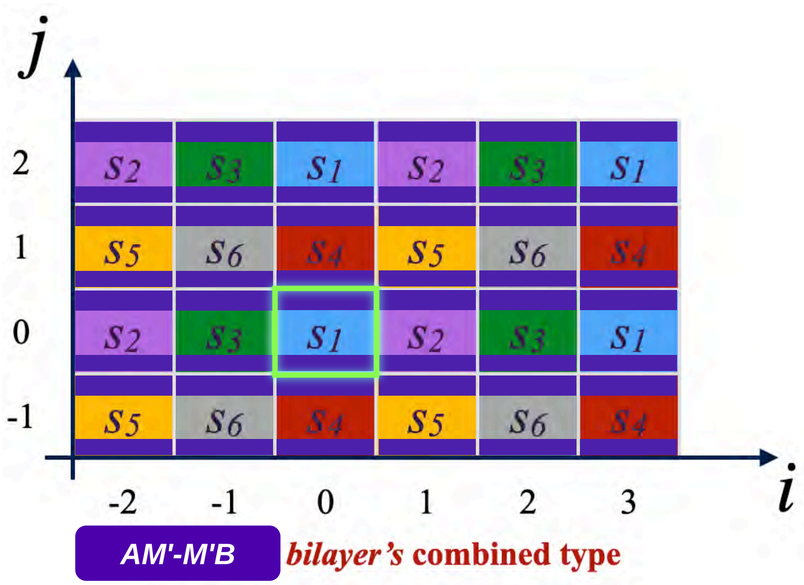


S6

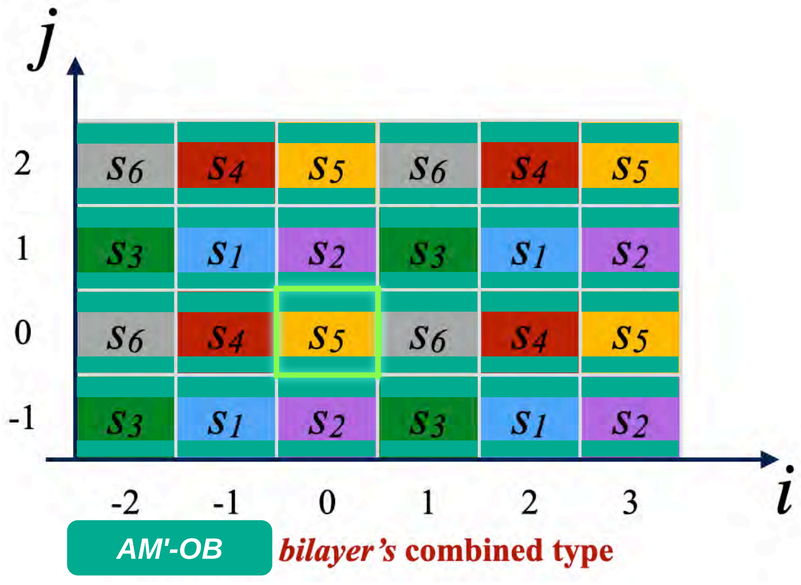




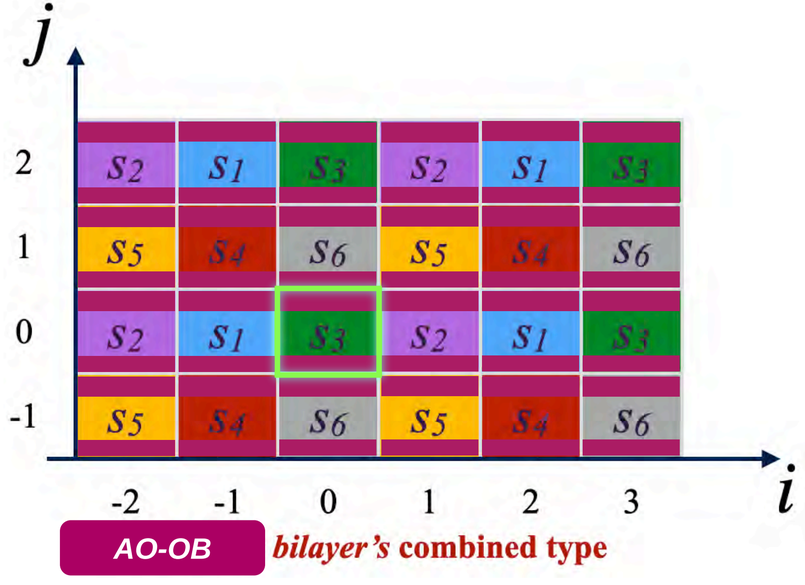
6 number of stacking configurations “s”



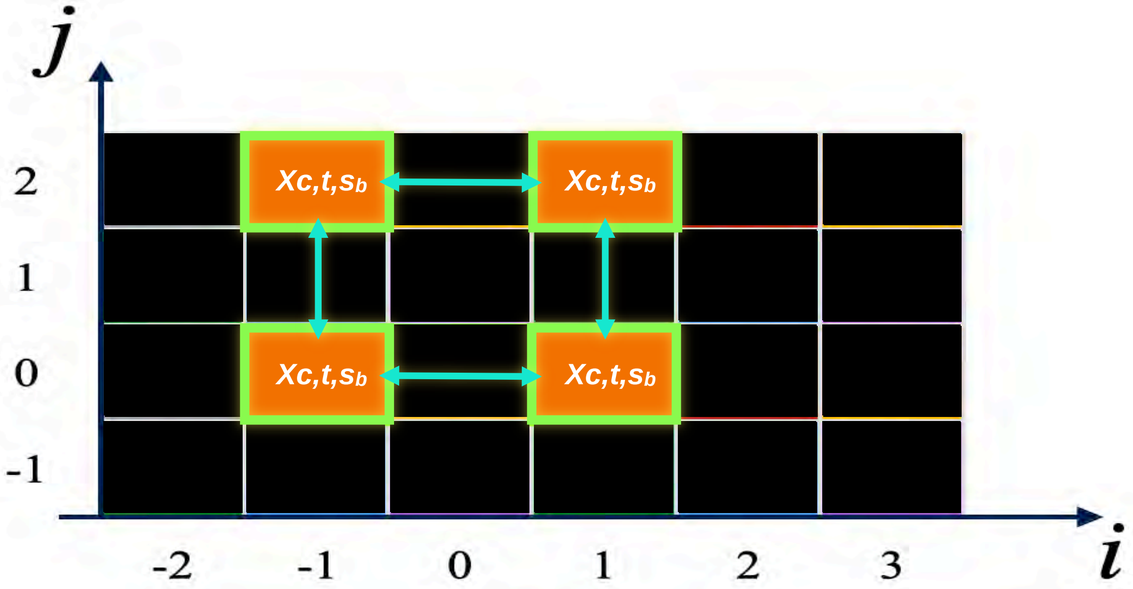
AM'-M'B *bilayer's* combined type



AM'-OB *bilayer's* combined type

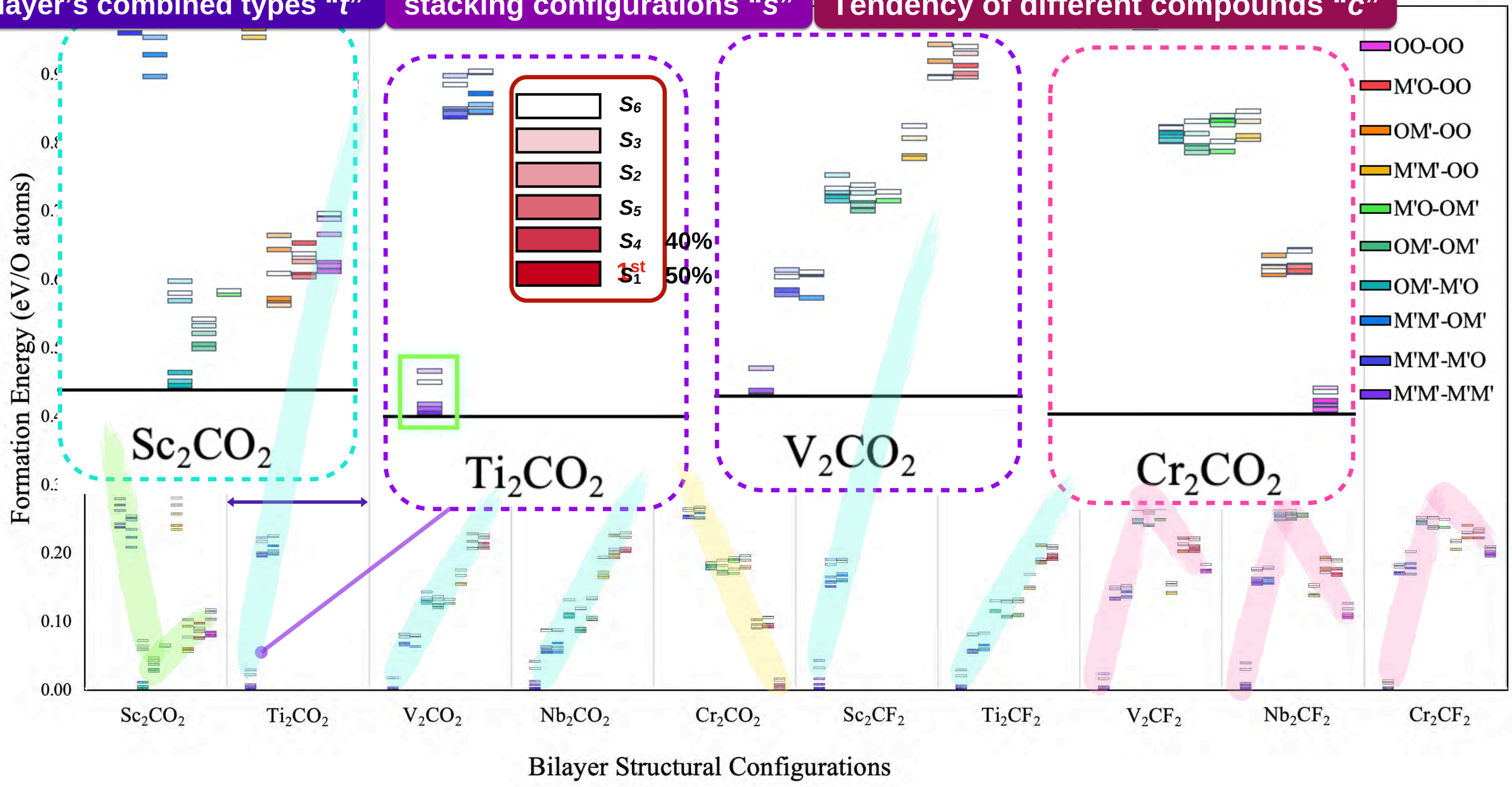


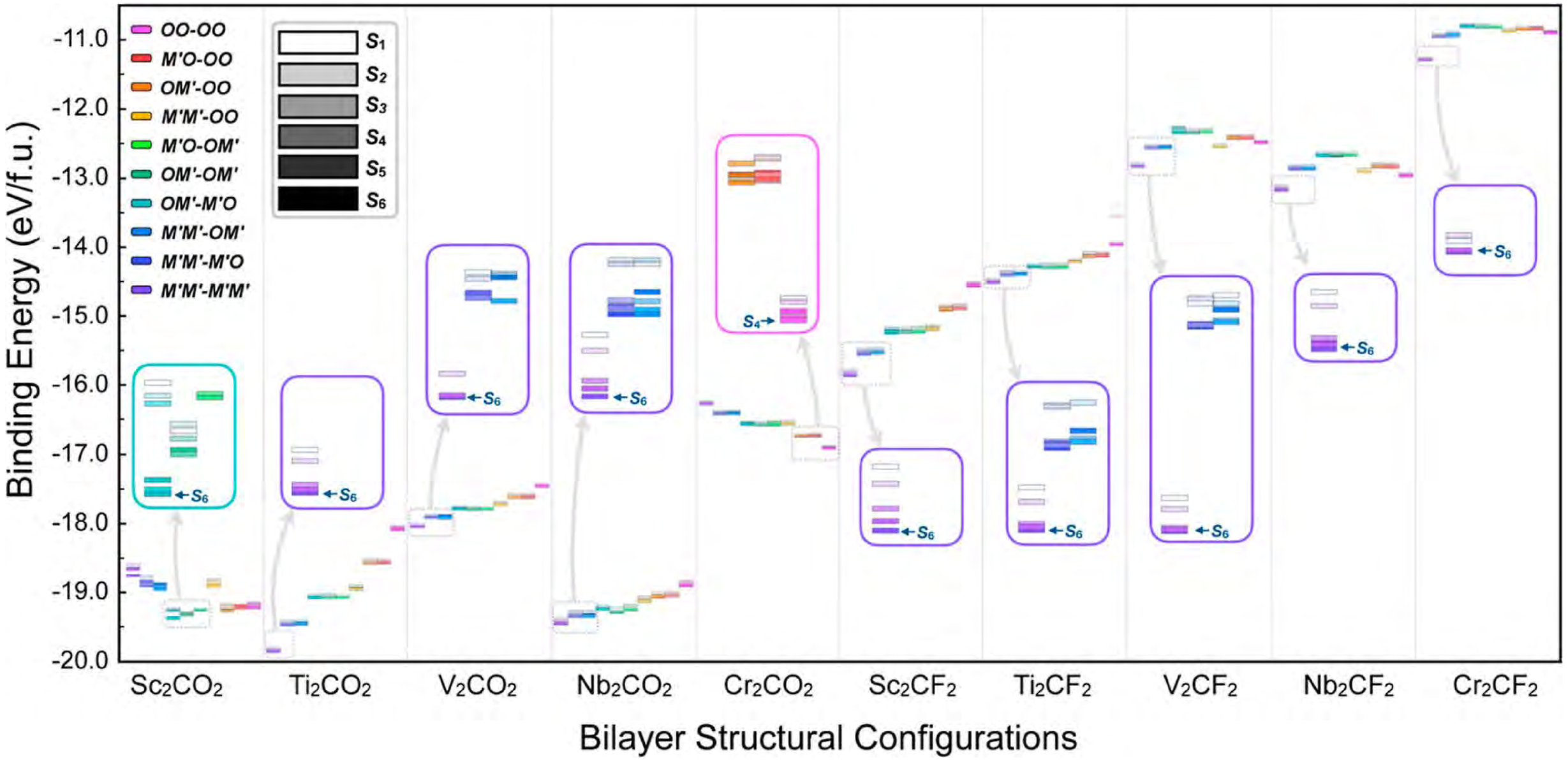
AO-OB *bilayer's* combined type



III. MXenes bilayer : Relative plot for all bilayer's formation energy

bilayer's combined types "*t*" | **stacking configurations "*s*"** | **Tendency of different compounds "*c*"**




OO-OO
M'O-OO
OM'-OO
M'M'-OO
M'O-OM'
OM'-OM'
OM'-M'O
M'M'-OM'
M'M'-M'O
M'M'-M'M'
S1
S2
S3
S4
S5
S6
Binding Energy (eV/f.u.)
-11.0
-12.0
-13.0
-14.0
-15.0
-16.0
-17.0
-18.0
-19.0
-20.0
Sc2CO2
Ti2CO2
V2CO2
Nb2CO2
Cr2CO2
Sc2CF2
Ti2CF2
V2CF2
Nb2CF2
Cr2CF2
Bilayer Structural Configurations

III. MXenes bilayer : Relative plot for all bilayer's formation energy

Compounds of the belayer ("*c*")	Bilayer's Combined type ("*t*")	Stacking configuration ("*s*")	Formation energy (eV)
Sc_2CO_2	*OM'-M'O*	s_1	-5.177
Ti_2CO_2	*M'M'-M'M'*	s_1	-5.415
V_2CO_2	*M'M'-M'M'*	s_1	-4.506
Nb_2CO_2	*M'M'-M'M'*	s_1	-5.211
Cr_2CO_2	*OO-OO*	s_5	-3.946
Sc_2CF_2	*M'M'-M'M'*	s_1	-6.296
Ti_2CF_2	*M'M'-M'M'*	s_1	-5.638
V_2CF_2	*M'M'-M'M'*	s_1	-4.804
Nb_2CF_2	*M'M'-M'M'*	s_1	
Cr_2CF_2	*M'M'-M'M'*	s_1	

Ti_2CO_2 compound,

***M'M'-M'M'* bilayer combined type,**

s_1 stacking configuration

IV. Li-ion applications

Material properties: candidates for Li-ion application

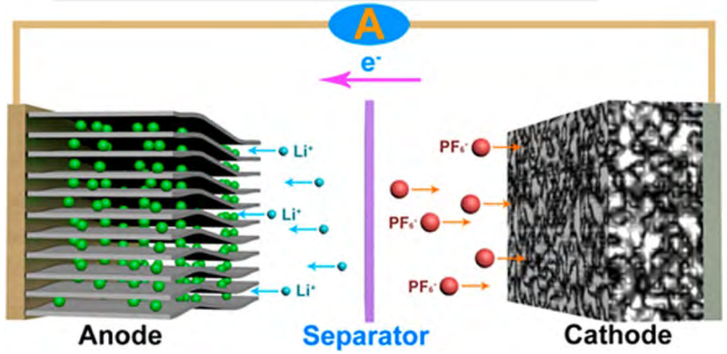
Good performance for energy storage material

Anode for Li-ion battery electrode

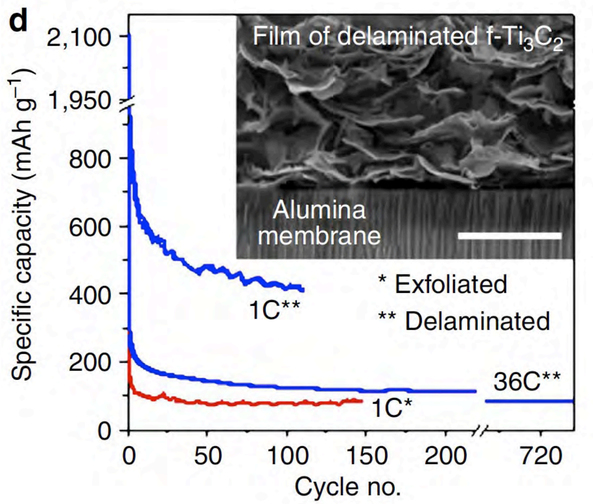
- **High capacitance**
- **Low diffusion barrier**
- **Positive voltage for Li-ion batteries**

Intercalation Process

Electrochemical route



Li-ion capacity of f-Ti_3C_2



Lukatskaya, M. R. et al.,Nature Energy (2017)

Key development of MXenes for Li-ion battery

- **Delaminated of multilayer**
- **Increase the interlayer spacing**
- **Increase the specific capacitance**
- **Decreasing of diffusion barrier**
- **Determined the voltage calculations**

IV. Li-ion applications : Diffusion properties of Ti_2CO_2 monolayer

Climbing image-nudged elastic band (CI-NEB)

The method works by optimizing a number of intermediate image along the reaction path connecting reactant and products

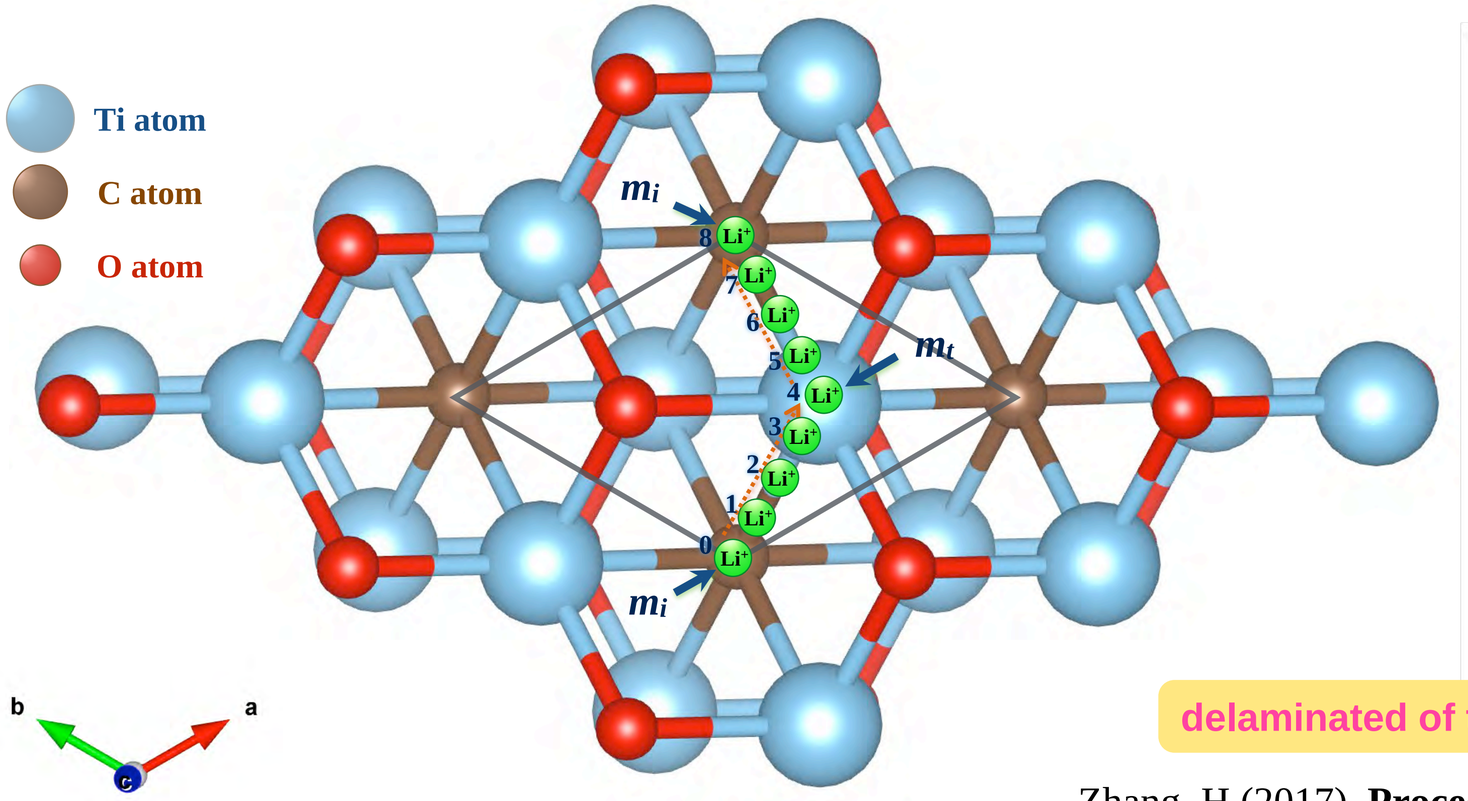
Each image find the lowest energy possible

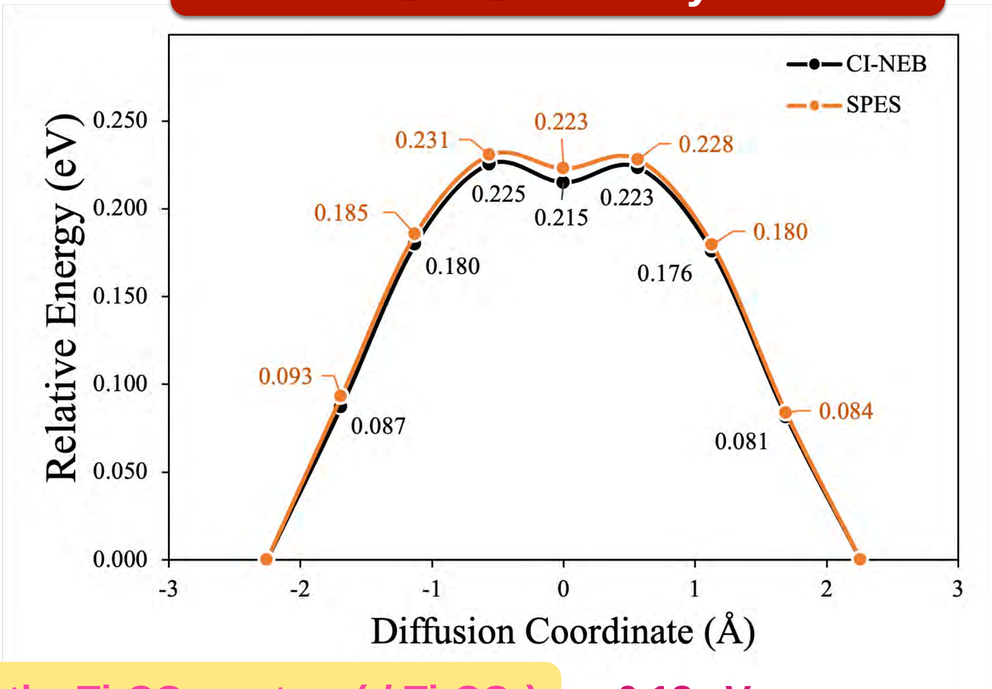
maintain equal spacing

Static potential energy (SPES)

Performs the calculation with fixed Li-ion in the x and y coordinates

Ti_2CO_2 monolayer

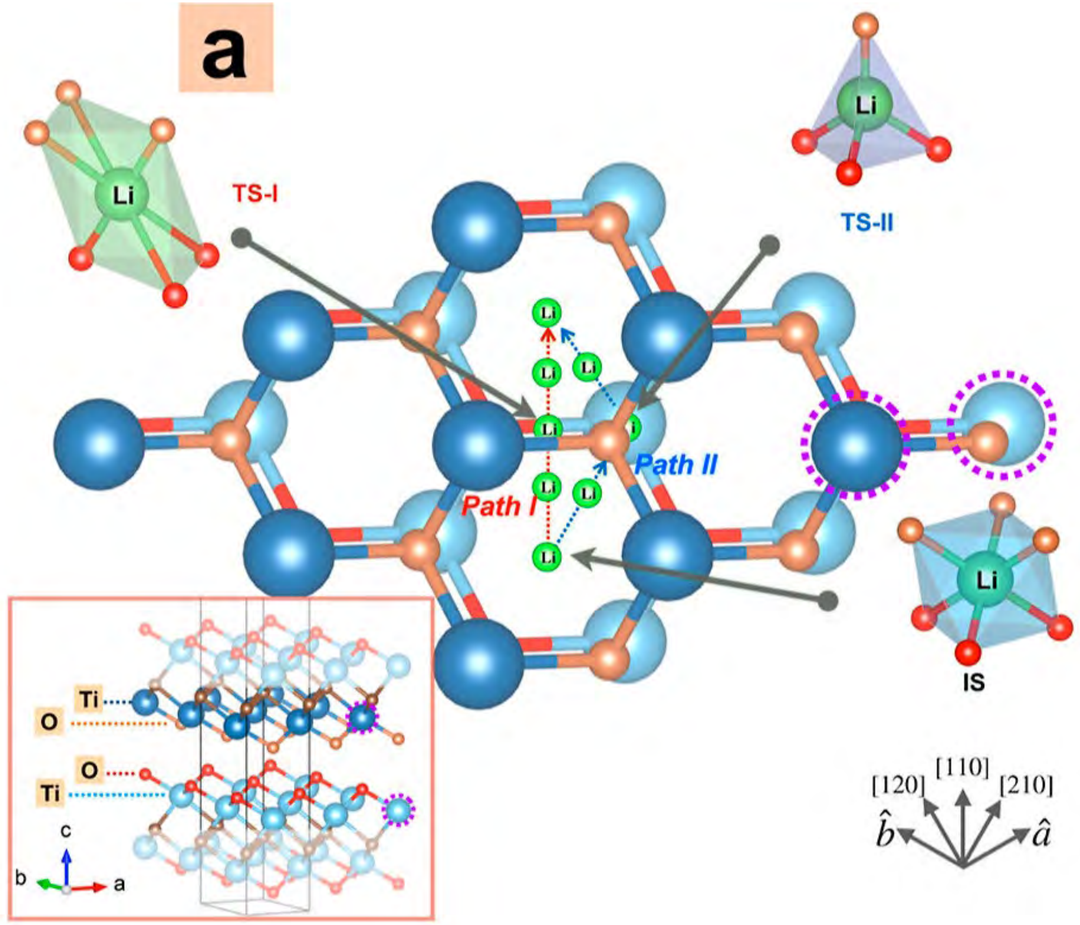




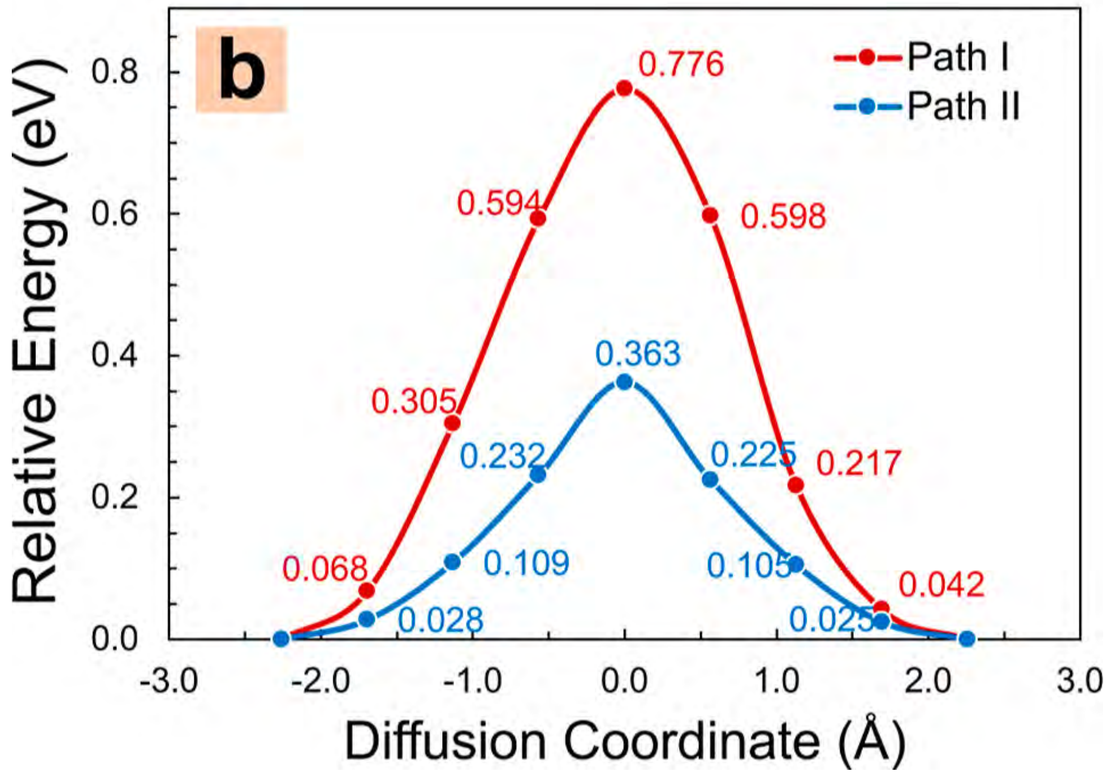
delaminated of the Ti_2CO_2 system (d-Ti_2CO_2) **~ 0.18 eV**

Zhang, H.(2017). **Proceedings of the National Academy of Sciences** 114: E11082

IV. Li-ion applications : Diffusion properties of Ti_2CO_2 bilayer



CI-NEB



Ti_2CO_2 Bilayer of the M'M'-M'M' combined type with "s_1" stacking configuration

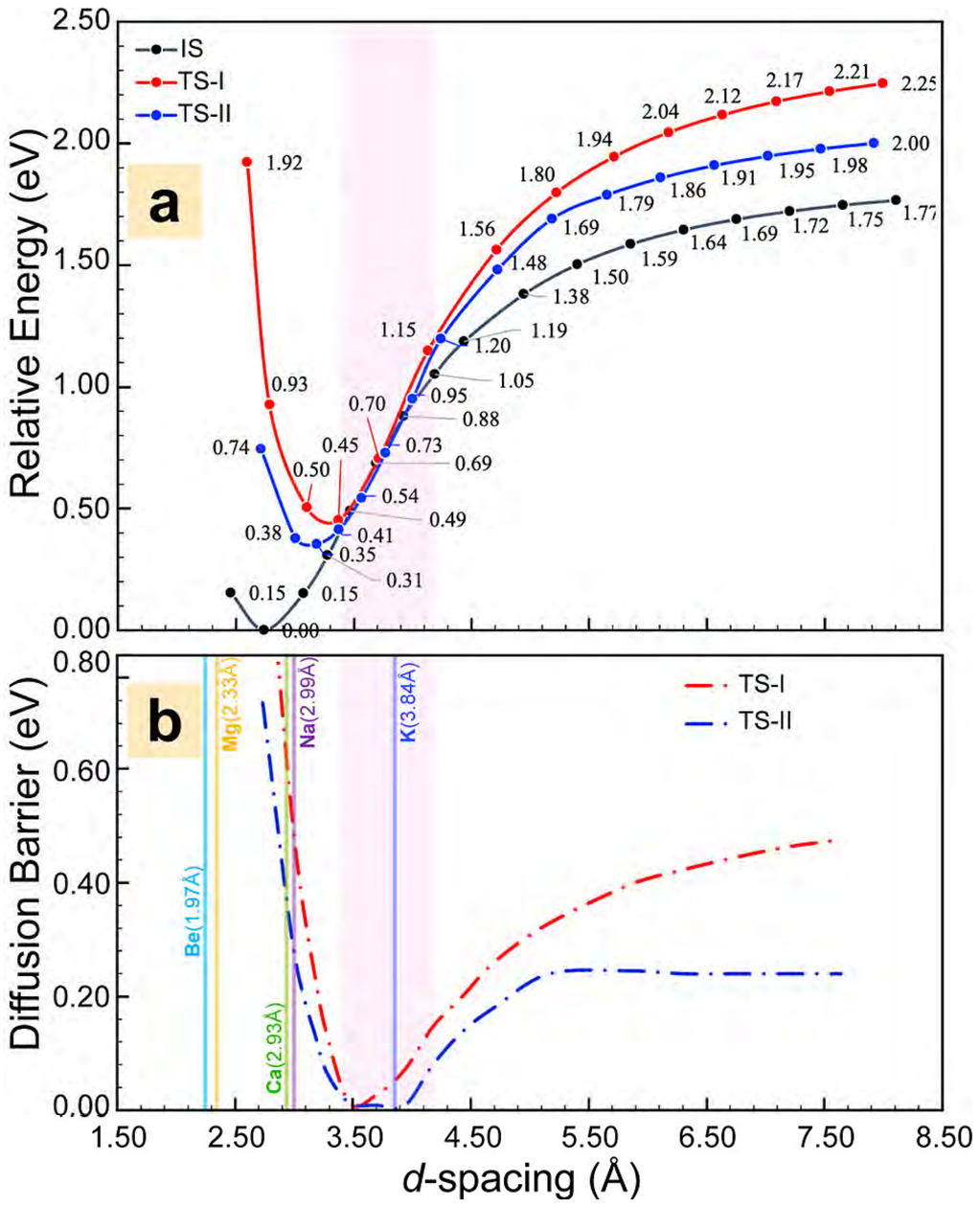
Overlying layer's Ti atom

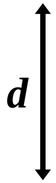
Overlying layer's O atom

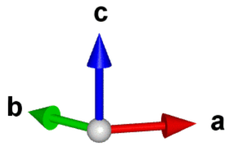
Underlying layer's Ti atom

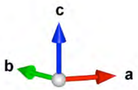
Underlying layer's O atom

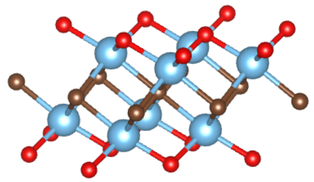
IV. Li-ion applications : *d*-spacing

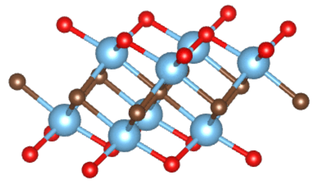


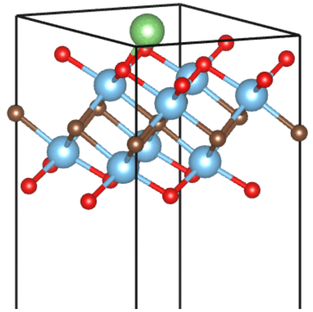


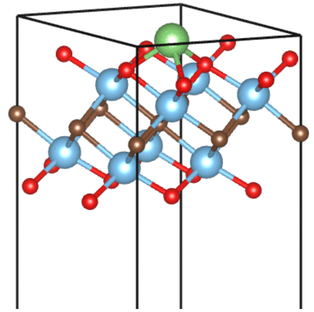












Initial state

Transition state of path I

Transition state of path II

Framework of increase interlayer spacing

To reduce the computation resource → ***b-IS***, ***b-TS I*** , ***b-TS II***

Interlayer spacing => *d*-spacing → **z-coordinate of both interface** (O atoms with non-interact with Li-atom)

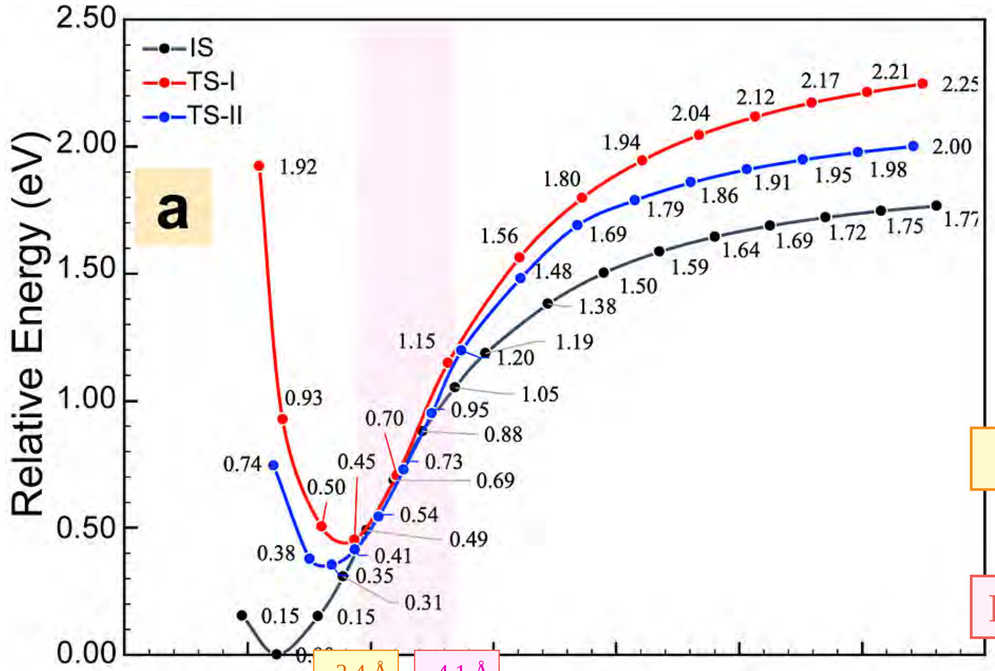
SPES method

Diffusion barrier ~ 0.01 eV

IV. Li-ion applications

Li-distance above underlying layer in z-coordinate

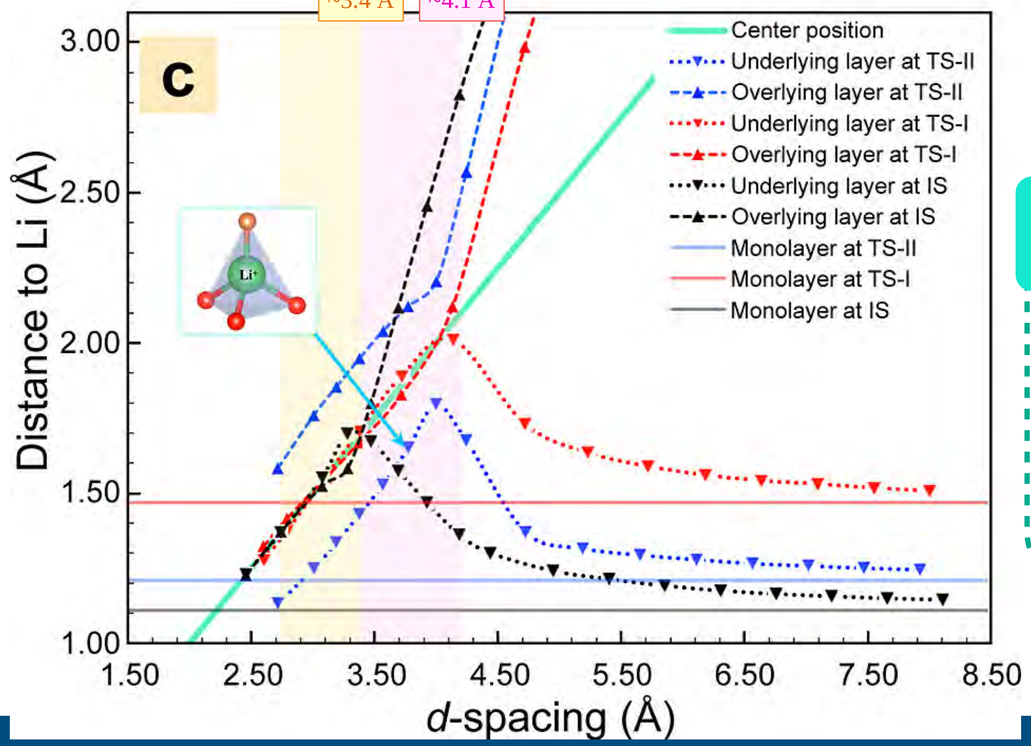
- Plot of three Li's sites → *b-IS*, *b-TS I* , *b-TS II*
- Green line is center distance



Region I ($d \sim 2.7 - 3.4$ Å)

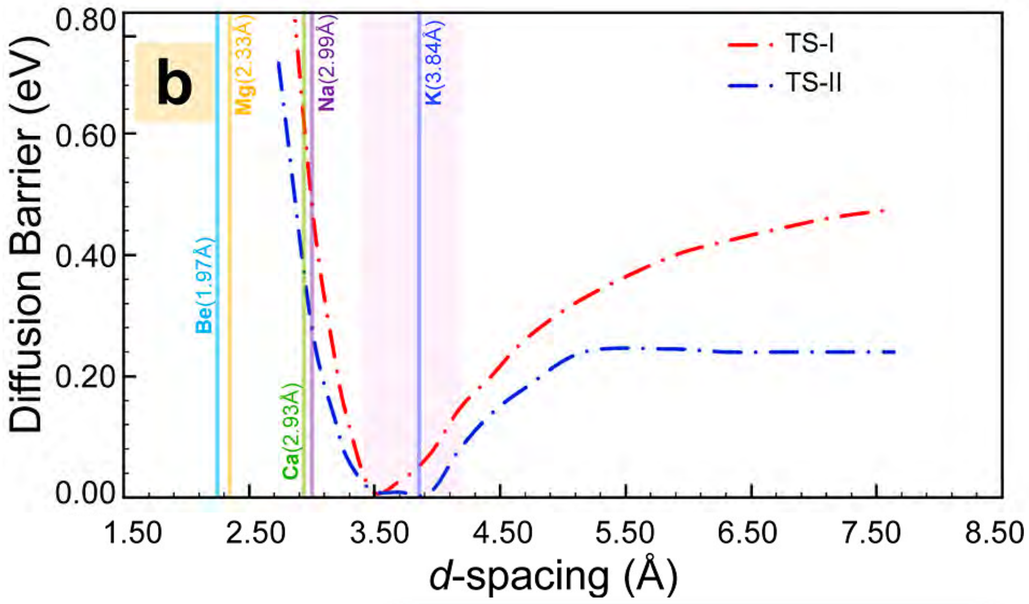
Region II ($d \sim 3.4 - 4.1$ Å)

Expansion of the interlayer spacing by metal intercalations



Co-intercalation framework

- Use primitive cell
- Insert of maximum of the co-intercalation



K and S co-intercalations are candidate

Relative diffusion rate (Selectivity) as a function of temperatures

Arrhenius equation

$$k = Ae^{\frac{-E_a}{RT}}$$

k = rate constant

A = pre-exponential factor

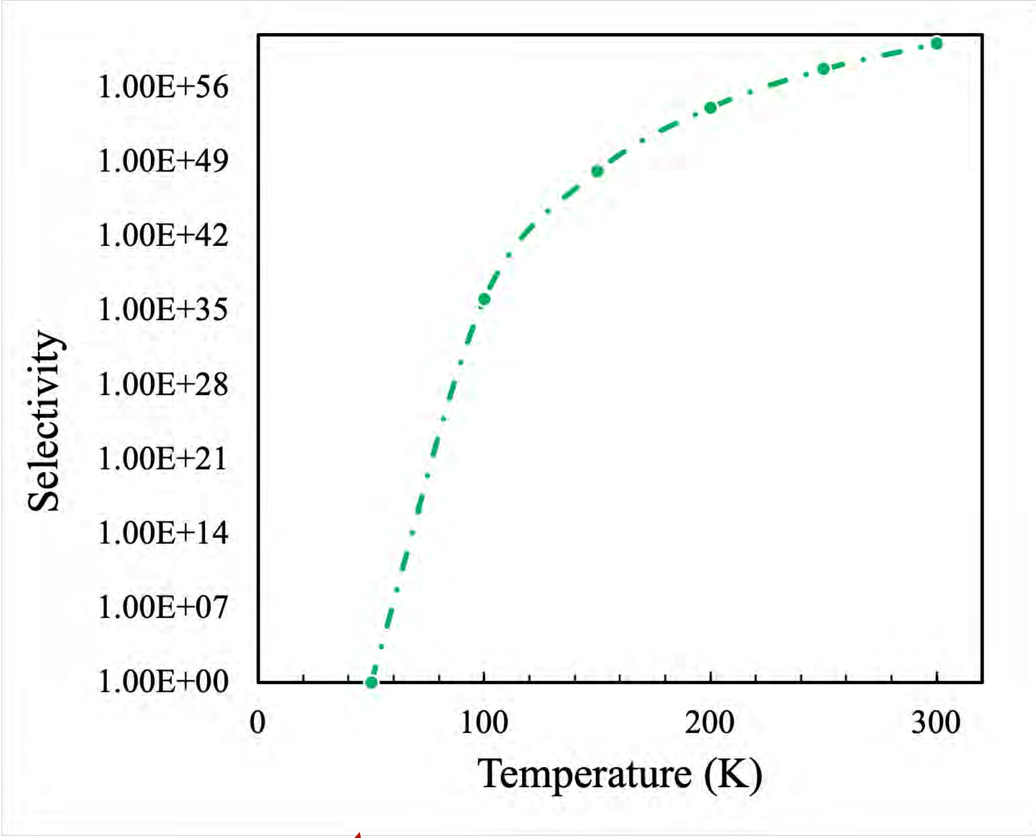
E_a = activation energy (in the same units as R*T)

R = universal gas constant

T = absolute temperature (in Kelvin)

Selectivity

$$S = \frac{k}{k_{ref}}$$



Selectivity of equilibrium structure of Li adsorption on the *b-IS* with 50K

(Diffusion barrier ~ 0.74 eV and correspond to d-spacing of ~ 2.71 Å)

Selectivity of Li-atom with different *d*-spacing as a function of temperatures

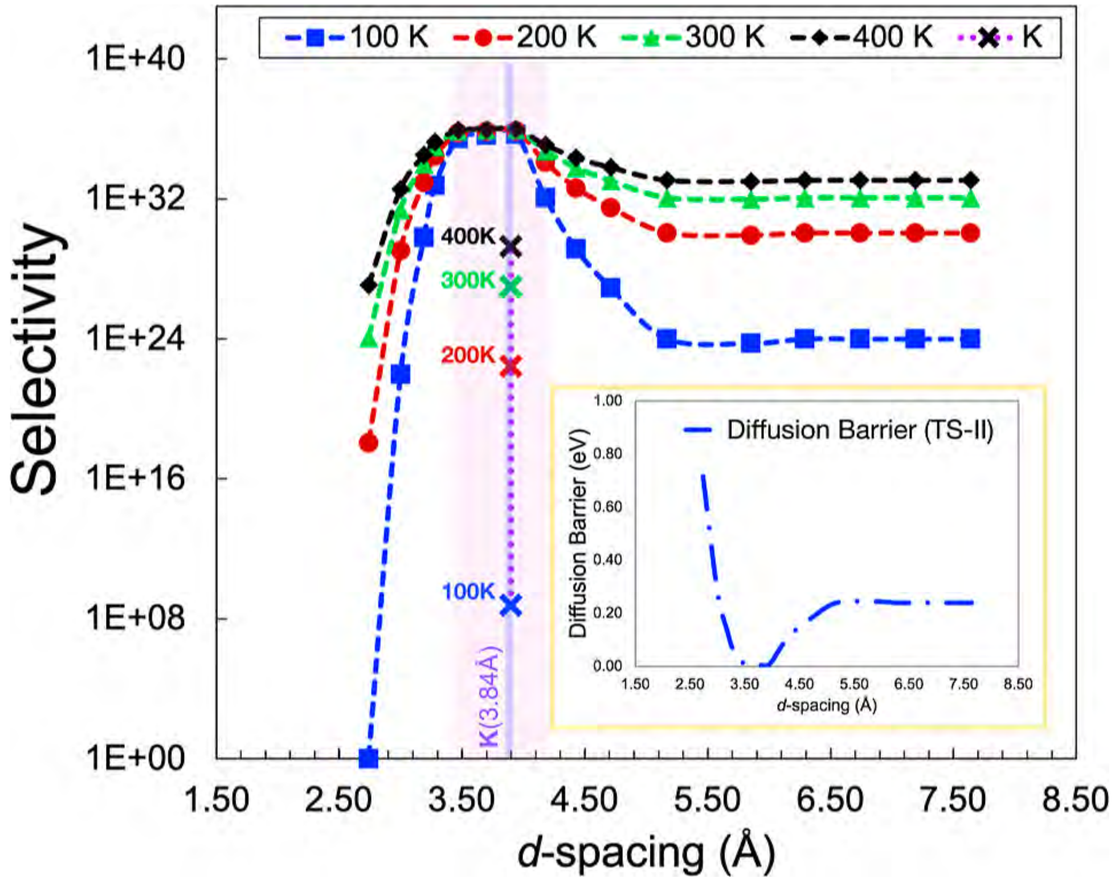
~~Region I ($d \sim 2.7 - 3.4$ Å)~~

The selectivity had a huge increase with *d*-spacing slightly increasing.

The selectivity is shown to be greatly enhanced for all examined temperatures.

Region II ($d \sim 3.4 - 4.1$ Å)

The selectivity characteristic is present identically at all temperatures



(Selectivity over equilibrium structure over the Li atom insertion at 50K)

Set the selectivity to relative with

Reaction rate of equilibrium structure of Li adsorption on the *b-IS* with 50K
(Diffusion barrier ~ 0.74 eV and correspond to d-spacing of ~ 2.71 Å)

with K co-intercalation

equilibrium of 221 supercell of K ~ 4.1 Å

Type of diffusion atom		Diffusion barrier (eV)
Li	Diffusion path I	0.109
	Diffusion path II	0.042
K	Diffusion path I	0.550
	Diffusion path II	0.542

Computation conditions

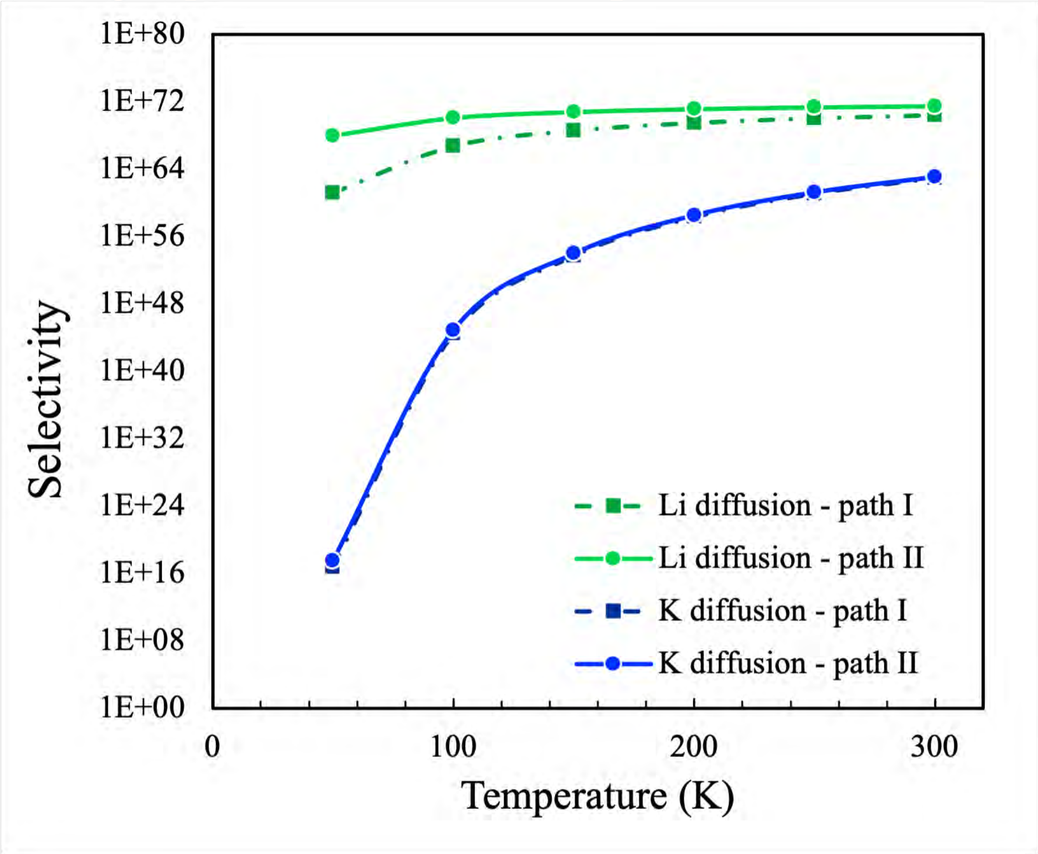
- Use supercell 2x2x1
- Insert 1 atom of the co-intercalation at the preferable site

Arrhenius equation

$$k = Ae^{\frac{-E_a}{RT}}$$

Reaction rate vs T of Li and K at the same *d*-spacing

(using equilibrium of 221 supercell of K ~ 4.1 Å)



K can be use as the co-intercalation

Set the selectivity to relative with

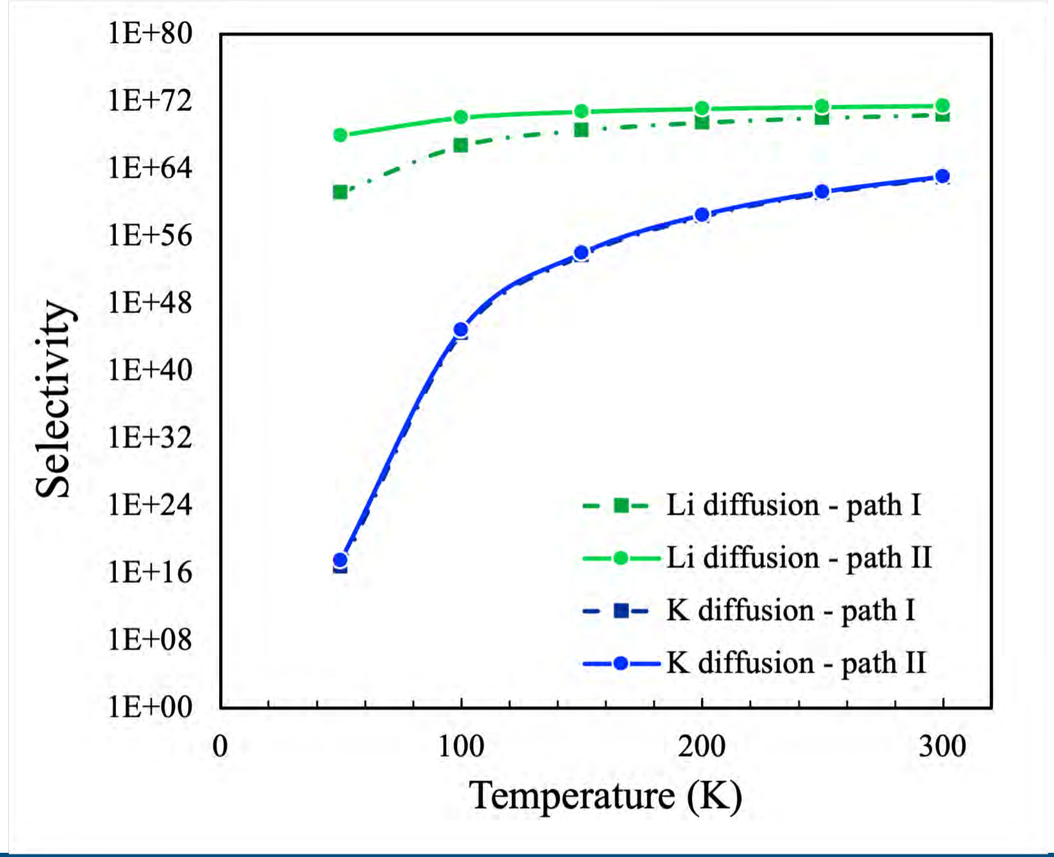
Reaction rate of equilibrium structure of Li adsorption on the *b-IS* with 50K
(Diffusion barrier ~ 0.74 eV and correspond to d-spacing of ~ 2.71 Å)

with K co-intercalation

equilibrium of 221 supercell of K ~ 4.1 Å

Type of diffusion atom		Diffusion barrier (eV)
Li	Diffusion path I	0.109
	Diffusion path II	0.042
K	Diffusion path I	0.550
	Diffusion path II	0.542

Reaction rate vs T of Li and K at the same *d*-spacing
(using equilibrium of 221 supercell of K ~ 4.1 Å)



V. Conclusion and Future direction

Studies of the monolayer

- Firstly, we discovered that, despite having a similar structure, M_2CT_2 exhibits different properties in different compounds in their family, such as the transition from semiconducting to conducting by changing the *T* and *M* elements.

- The majority of the ***M'M'***, ***M'O***, and ***OO*** models for the M_2CT_2 MXenes, respectively, reveal the most preferred structure according to the evaluation of the formation energy.

Bilayer

- The characteristic of the $\boldsymbol{s_1}$ stacking configuration and ***M'M'-M'M'*** bilayer combined type emerging as the most preferred configuration among all the combined types of the M_2CT_2 bilayers.

- This study will draw attention to the fact that the properties of the M_2CT_2 MXenes multilayer can be manipulated by regulating the structural arrangements in addition to the monolayer.

Li-ion applications

- The computed diffusion barrier for the CI-NEB methods is 0.776 eV and 0.363 eV, for the transition paths I and II, respectively.
- The Li-ion diffusion barrier for the intrinsic Ti_2CO_2 bilayer is 0.363 eV and found to be significantly low (~0.01 eV) with interlayer spacings between 3.40 Å and 4.10 Å.
- At a certain interlayer distance, Li atom is neglected by both Ti_2CO_2 layers at the bilayer interface.
- Interestingly, the potassium co-intercalation offers the opportunity to alter the Ti_2CO_2 bilayer's interlayer spacing to cover the ultra-low diffusion barrier characteristic and maintaining its position during Li diffusion.
- For this reason, in terms of enhancing the charging rate in the LIB application, potassium co-intercalation may be suggested.